

Robert M. Haralick  
 Department of Electrical Engineering  
 Department of Computer Science  
 University of Kansas  
 Lawrence, Kansas 66045

ABSTRACT

In this survey we review the image processing literature on the various approaches and models investigators have used for textures. These include statistical approaches of autocorrelation function, optical transforms, digital transforms, textural edgeness, structural element, gray tone co-occurrence, run lengths, and auto-regressive models. We discuss and generalize some structural approaches to texture based on more complex primitives than gray tone. We conclude with some structural-statistical generalizations which apply the statistical techniques to the structural primitives.

I. INTRODUCTION

Texture is an important characteristic for the analysis of many types of images. It can be seen in all images from multi-spectral scanner images obtained from aircraft or satellite platforms (which the remote sensing community analyzes) to microscopic images of cell cultures or tissue samples (which the bio-medical community analyzes). Despite its importance and ubiquity in image data, a precise definition of texture does not exist. In this paper we survey and generalize some of the extraction techniques and models which investigators have been using to measure textural properties.

The image texture we consider is non-figurative and cellular. We think of this kind of texture as an organized area phenomena. When it is decomposable, it has two basic dimensions on which it may be described. The first dimension is for describing the primitives out of which the image texture is composed and the second dimension is for the description of the spatial dependence or interaction between the primitives of an image texture. The first dimension is concerned with tonal primitives or local properties, and the second dimension is concerned with the spatial organization of the tonal primitives.

Tonal primitives are regions with tonal properties. The tonal primitive can be described in terms such as the average tone, or maximum and minimum tone of its region. The region is a maximally connected set of pixels having a given tonal property. The tonal region can be evaluated in terms of its area and shape. The tonal primitive includes both its gray tone and tonal region properties.

An image texture is described by the number and types of its primitives and the spatial organization or layout of its primitives. The spatial organization may be random, may have a pairwise dependence of one primitive on a neighboring primitive, or may have a dependence of  $n$  primitives at a time. The dependence may be structural, probabilistic, or functional (like a linear dependence).

Image texture can be qualitatively evaluated as having one or more of the following properties: fine, coarse, smooth, granulated, rippled, mottled, irregular, random, lineated, or hummocky. Each of these adjectives translates into some property of the tonal primitives and the spatial interaction between the tonal primitives. Unfortunately, few experiments have

been done attempting to map semantic meaning into precise properties of tonal primitives and their spatial distributional properties.

To objectively use the tone and textural pattern elements, the concepts of tonal and textural feature must be explicitly defined. With an explicit definition, we discover that tone and texture are not independent concepts. They bear an inextricable relationship to one another very much like the relation between a particle and a wave. There really is nothing that is only particle or only wave. Whatever exists has both particle and wave properties and depending on the situation, the particle or wave properties may predominate. Similarly, in the image context, tone and texture are always there, although at times one property can dominate the other and we tend to speak of only tone or only texture. Hence, when we make an explicit definition of tone and texture, we are not defining two concepts: we are defining one tone-texture concept.

The basic inter-relationships in the tone-texture concept are the following. When a small-area patch of an image has little variation of tonal primitives, the dominant property of that area is tone. When a small-area patch has wide variation of tonal primitives, the dominant property of that area is texture. Crucial in this distinction are the size of the small-area patch, the relative sizes and types of tonal primitives, and the number and placement or arrangement of the distinguishable primitives. As the number of distinguishable tonal primitives decreases, the tonal properties will predominate. In fact, when the small-area patch is only the size of one resolution cell, so that there is only one discrete feature, the only property present is simple gray tone. As the number of distinguishable tonal primitives increases within the small-area patch, the texture property will dominate. When the spatial pattern in the tonal primitives is random and the gray tone variation between primitives is wide, a fine texture results. As the spatial pattern becomes more definite and the tonal regions involve more and more resolution cells, a coarser texture results<sup>64</sup>.

In summary, to characterize texture, we must characterize the tonal primitive properties as well as characterize the spatial inter-relationships between them. This implies that texture-tone is really a two-layered structure, the first layer having to do with specifying the local properties which manifest themselves in tonal primitives and the second layer having to do with specifying the organization among the tonal primitives. We, therefore, would expect that methods designed to characterize texture would have parts devoted to analyzing each of these aspects of texture. In the review of the work done to date, we will discover that each of the existing methods tends to emphasize one or the other aspect and tends not to treat each aspect equally.

## II. REVIEW OF THE LITERATURE ON TEXTURE MODELS

There have been eight statistical approaches to the measurement and characterization of image texture: autocorrelation functions, optical transforms, digital transforms, textural edgeness, structural elements, spatial gray tone co-occurrence probabilities, gray tone run lengths, and auto-regressive models. An early review of some of these approaches is given by

<sup>36</sup> Hawkins. The first three of these approaches are related in that they all measure spatial frequency directly or indirectly. Spatial frequency is related to texture because fine textures are rich in high spatial frequencies while coarse textures are rich in low spatial frequencies.

An alternative to viewing texture as spatial frequency distribution is to view texture as amount of edge per unit area. Coarse textures have a small number of edges per unit area. Fine textures have a high number of edges per unit area.

The structural element approach of Serra <sup>78</sup> and <sup>49</sup> Matheron uses a matching procedure to detect the spatial regularity of shapes called structural elements in a binary image. When the structural elements themselves are single resolution cells, the information provided by this approach is the autocorrelation function of the binary image. By using larger and more complex shapes, a more generalized autocorrelation can be computed.

The gray tone spatial dependence approach characterizes texture by the co-occurrence of its gray tones. Coarse textures are those for which the distribution changes only slightly with distance and fine textures are those for which the distribution changes rapidly with distance.

The gray level run length approach characterizes coarse textures as having many pixels in an average constant gray tone run and fine textures as having few pixels in an average gray tone run.

The auto-regressive model is a way to use linear estimates of a pixel's gray tone given the gray tones in a neighborhood containing it in order to characterize texture. For coarse textures, the coefficients will all be similar. For fine textures, the coefficients will have wide variation.

The power of the spatial frequency approach to texture is the familiarity we have with these concepts. However, one of the inherent problems is in regard to gray tone calibration of the image. The procedures are not invariant under even a linear translation of gray tone. To compensate for this, probability quantizing can be employed. But, the price paid for the invariance of the quantized images under monotonic gray tone transformations is the resulting loss of gray tone precision in the quantized image. Weszka, Dyer, and Rosenfeld <sup>92</sup> compare the effectiveness of some of these techniques for terrain classification. They conclude that spatial frequency approaches perform significantly poorer than the other approaches.

The power of the structural element approach is that it emphasizes the shape aspects of the tonal primitives. Its weakness is that it can only do so for binary images.

The power of the co-occurrence approach is that it characterizes the spatial inter-relationships of the gray tones in a textural pattern and can do so in a way that is invariant under monotonic gray tone

transformations. Its weakness is that it does not capture the shape aspects of the tonal primitives. Hence, it is not likely to work well for textures composed of large-area primitives.

The power of the auto-regressive linear estimator approach is that it is easy to use the estimator in a mode which synthesizes textures from any initially given linear estimator. In this sense, the auto-regressive approach is sufficient to capture everything about a texture. Its weakness is that the textures it can characterize are likely to consist mostly of micro-textures.

### II.1 The Autocorrelation Function and Texture

From one point of view, texture relates to the spatial size of the tonal primitives on an image. Tonal primitives of larger size are indicative of coarser textures; tonal primitives of smaller size are indicative of finer textures. The autocorrelation function is a feature which tells about the size of the tonal primitives.

We describe the autocorrelation function with the help of a thought experiment. Consider two image transparencies which are exact copies of one another. Overlay one transparency on top of the other and with a uniform source of light, measure the average light transmitted through the double transparency. Now, translate one transparency relative to the other and measure only the average light transmitted through the portion of the image where one transparency overlaps the other. A graph of these measurements as a function of the  $(x,y)$  translated positions and normalized with respect to the  $(0,0)$  translation depicts the two-dimensional autocorrelation function of the image transparency.

Let  $I(u,v)$  denote the transmission of an image transparency at position  $(u,v)$ . We assume that outside some bounded rectangular region  $0 \leq u \leq L_x$  and  $0 \leq v \leq L_y$  the image transmission is zero. Let  $(x,y)$  denote the  $x$ -translation and  $y$ -translation, respectively. The autocorrelation function for the image transparency  $d$  is formally defined by:

$$\rho(x,y) = \frac{\frac{1}{(L_x - |x|)(L_y - |y|)} \iint_{-\infty}^{\infty} I(u,v)I(u+x,v+y)du dv}{\frac{1}{L_x L_y} \iint_{-\infty}^{\infty} I^2(u,v)du dv}$$

$$|x| < L_x \quad \text{and} \quad |y| < L_y$$

If the tonal primitives on the image are relatively large, then the autocorrelation will drop off slowly with distance. If the tonal primitives are small, then the autocorrelation will drop off quickly with distance. To the extent that the tonal primitives are spatially periodic, the autocorrelation function will drop off and rise again in a periodic manner. The relationship between the autocorrelation function and the power spectral density function is well known: they are Fourier Transforms of one another (Yaglom <sup>95</sup>).

The tonal primitive in the autocorrelation model is the gray tone. The spatial organization is characterized by the correlation coefficient which is a measure of the linear dependence one pixel has on another.

An experiment was carried out by Kaizer<sup>41</sup> to see if the autocorrelation function had any relationship to the texture which photo-interpreters see in images. He used a series of seven aerial photographs of an Arctic region (see Figure 1) and determined the autocorrelation function of the images with a spatial correlator which worked in a manner similar to the one envisioned in our thought experiment. Kaizer assumed the autocorrelation function was circularly symmetric and computed it only as a function of radial distance. Then for each image, he found the distance  $d$  such that the autocorrelation function  $\rho$  at  $d$  took the value

$$\frac{1}{e}: \rho(d) = \frac{1}{e}$$

Kaizer then asked 20 subjects to rank the seven images on a scale from fine detail to coarse detail. He correlated the rankings with the distances corresponding to the  $(\frac{1}{e})$ th value of the autocorrelation function. He found a correlation coefficient of .99. This established that at least for his data set, the autocorrelation function and the subjects were measuring the same kind of textural features.

Kaizer noticed, however, that even though there was a high degree of correlation between  $\rho^{-1}(\frac{1}{e})$  and subject rankings, some subjects put first what  $\rho^{-1}(\frac{1}{e})$  put fifth. Upon further investigation, he discovered that a relatively flat background (indicative of high frequency or fine texture) can be interpreted as a fine textured or coarse textured area. This phenomena is not unusual and actually points out a fundamental characteristic of texture: it cannot be analyzed without a reference frame of tonal primitive being stated or implied. For any smooth gray tone surface, there exists a scale such that when the surface is examined, it has no texture. Then as resolution increases, it takes on a fine texture and then a coarse texture. In Kaizer's situation, the resolution of his spatial correlator was not good enough to pick up the fine texture which some of his subjects did in an area which had a weak but fine texture.

## II.2 Optical Processing Methods and Texture

Edward O'Neill's article<sup>61</sup> on spatial filtering introduced the engineering community to the fact that optical systems can perform filtering of the kind used in communication systems. In the case of the optical systems, however, the filtering is two-dimensional. The basis for the filtering capability of optical systems lies in the fact that the light amplitude distributions at the front and back focal planes of a lens are Fourier Transforms of one another. The light distribution produced by the lens is more commonly known as the Fraunhofer diffraction pattern. Thus, optical methods facilitate two-dimensional frequency analysis of images.

The paper by Cutrona et al.<sup>12</sup> provides a good review of optical processing methods for the interested reader. More recent books by Goodman<sup>22</sup>, Preston<sup>66</sup>, and Shulman<sup>81</sup> comprehensively survey the area.

In this section we describe the experiments done by Lendaris and Stanley, and others using optical processing methods on aerial or satellite imagery.

Lendaris and Stanley<sup>45,46</sup> illuminated small circular sections of low altitude aerial photography and used the Fraunhofer diffraction pattern as features for identifying the sections. The circular sections represented a circular area on the ground of 750 feet. The major category distinction they were interested in making was man-made versus non man-made. They further subdivided the man-made category into roads, road intersections, buildings, and orchards.

The pattern vectors they used from the diffraction pattern consisted of 40 components. Twenty components were averages of the energy in annular regions of the diffraction pattern and 20 were averages of the energy in  $9^{\circ}$  wedges of the diffraction pattern. They obtained over 90 percent identification accuracy.

Egbert et al.<sup>17</sup> used an optical processing system to examine the texture on LANDSAT imagery over Kansas. They used circular areas corresponding to a ground diameter of about 23 miles and looked at the diffraction patterns for the areas when they were snow covered and when they were not snow covered. They used a Recognition System diffraction pattern sampling unit having 23 sector wedges and 32 annular rings to sample and measure the diffraction patterns. They were able to interpret the resulting angular orientation graphs in terms of dominant drainage patterns and roads, but were not able to interpret the spatial frequency graphs which all seem to have had the same character: the higher the spatial frequency, the less the energy in that frequency band.

Honeywell Systems and Research Division has done work using optical processing on aerial images to identify species of trees. Using imagery obtained from Itasca State Park in northern Minnesota, photo-interpreters identified five (mixture) species of trees on the basis of the texture: Upland Hardwoods, Jack pine overstory/Aspen understory, Aspen overstory/Upland Hardwoods understory, Red pine overstory/Aspen understory, and Aspen. They achieved classification accuracy of over 90 percent.

## II.3 Digital Transform Methods and Texture

In the digital transform method of texture analysis, the digital image is typically divided into a set of non-overlapping small square subimages. Suppose the size of the subimage is  $n \times n$  resolution cells, then the  $n^2$  gray tones in the subimage can be thought of as the  $n^2$  components of an  $n^2$ -dimensional vector. The set of the subimages then constitutes a set of  $n^2$ -dimensional vectors. In the transform technique, each of these vectors is re-expressed in a new coordinate system. The Fourier Transform uses the sine-cosine basis set. The Hadamard Transform uses the Walsh function basis set, etc. The point to the transformation is that the basis vectors of the new coordinate system have an interpretation that relates to spatial frequency or sequency and since frequency is a close relative of texture, such transformations can be useful.

The tonal primitive in spatial frequency (sequency) models is the gray tone. The spatial organization is characterized by the kind of linear dependence which measures projection lengths.

Gramenopoulos<sup>23</sup> used a transform technique employing the sine-cosine basis vectors (and implemented it with the FFT algorithm) on ERTS imagery. He was interested in the power of texture and spatial pattern to do terrain type recognition. He used subimages of 32 by 32 resolution cells and found that on a Phoenix, Arizona LANDSAT image 1049-17324-5, spatial frequencies larger than 3.5 cycles/km and smaller than 5.9 cycles/km contain most of the information needed to discriminate between terrain types. His terrain classes were: clouds, water, desert, farms, mountains, urban, riverbed, and cloud shadows. He achieved an overall identification accuracy of 87 percent.

Horning and Smith<sup>37</sup> have done work similar to Gramenopoulos, but with aerial multispectral scanner imagery instead of LANDSAT imagery.

Kirvida and Johnson<sup>43</sup> compared the fast Fourier, Hadamard, and Slant Transforms for textural features on LANDSAT imagery over Minnesota. They used 8 x 8 sub-images and five categories: Hardwoods, Conifers, Open, City, Water. Using only spectral information, they obtained 74 percent correct identification accuracy. When they added textural information, they increased their identification accuracy to 99 percent. They found little difference between the different transform methods. See also Kirvida<sup>42</sup>.

Maurer<sup>51</sup> obtained encouraging results classifying crops from low altitude color photography on the basis of a one-dimensional Fourier series taken on a direction orthogonal to the rows.

Bajcsy and Lieberman<sup>3,4</sup> divided the image into square windows and used the two-dimensional power spectrum of each window. They expressed the power spectrum in a polar coordinate system of radius  $r$  versus angle  $\theta$ , treating the power spectrum as two independent one-dimensional functions of  $r$  and  $\theta$ . Directional textures tend to have peaks in the power spectrum as a function of  $\theta$ . Blob-like textures tend to have peaks in the power spectrum as a function of  $r$ . They showed that texture gradients can be measured by locating the trends of relative maxima of  $r$  or  $\theta$  as a function of the position of the window whose power spectrum is being taken.

#### II.4 Textural Edgeness

The autocorrelation function, the optical transforms, and digital transforms basically all reference texture to spatial frequency. Rosenfeld and Troy<sup>77</sup> and Rosenfeld and Thurston<sup>76</sup> conceive of texture not in terms of spatial frequency but in terms of edgeness per unit area. An edge passing through a resolution cell can be detected by comparing the values for local properties obtained in pairs of nonoverlapping neighborhoods bordering the resolution cell. To detect microedges, small neighborhoods can be used. To detect macroedges, large neighborhoods can be used.

The local property which Rosenfeld and Thurston suggested was the quick Roberts gradient (the sum of the absolute value of the differences between diagonally opposite neighboring pixels). Thus, a measure of texture for any subimage can be obtained by computing the Roberts gradient image for the subimage and from it determining the average value of the gradient in the subimage.

Sutton and Hall<sup>83</sup> extend Rosenfeld and Thurston's idea by making the gradient a function of the distance between the pixels. Thus, for every distance  $d$

and subimage  $I$  defined over neighborhood  $N$ , they compute:

$$g(d) = \sum_{(i,j) \in N} \{ |I(i,j) - I(i+d,j)| + |I(i,j) - I(i-d,j)| + |I(i,j) - I(i,j+d)| + |I(i,j) - I(i,j-d)| \}$$

The curve of  $g(d)$  is like the graph of the minus autocorrelation function translated vertically.

Sutton and Hall applied this textural measure in a pulmonary disease identification experiment and obtained identification accuracy in the 80 percentile range for discriminating between normal and abnormal lungs when using a 128 x 128 subimage.

Triendl<sup>90</sup> measures degree of edgeness by filtering the image with a 3 x 3 averaging filter and a 3 x 3 Laplacian filter. The two resulting filtered images are then smoothed with an 11 x 11 smoothing filter. The two values of average tone and roughness obtained from the low and high frequency filtered image can be used as textural features.

Hsu<sup>38</sup> determines textural edgeness by computing gradient-like measures for the gray tones in a neighborhood. If  $N$  denotes the set of resolution cells in a neighborhood about a pixel, and  $g_c$  is the gray tone of the center pixel,  $\mu$  is the mean gray tone in the neighborhood and  $\rho$  is a metric, then Hsu suggests that:

$$\sum_{(i,j) \in N} \rho(I(i,j), \mu), \quad \sum_{(i,j) \in N} \rho(I(i,j), g_c), \quad \text{and} \quad \rho(\mu, g_c)$$

are all appropriate measures for textural edgeness at a pixel.

#### II.5 Texture and Mathematical Morphology

A structural element and filtering approach to texture on binary images was proposed by Matheron<sup>49</sup> and Serra<sup>80</sup>. Their basic idea is to define a structural element as a set of resolution cells constituting a specific shape such as a line or a square and to generate a new binary image by translating the structural element through the image and eroding by the structural element the figures formed by contiguous resolution cells having the value 1. The textural features can be obtained from the new binary image by counting the number of resolution cells having the value 1. The structural element approach of Serra and Matheron is the basis of the Leitz texture analyses. (Müller and Herman<sup>59</sup>, Müller<sup>58</sup>, Serra<sup>78</sup>). The approach has found wide application in the quantitative analysis of micro-structures in materials science and biology.

To make these ideas precise, we first define the translate of a set. Let  $Z$  be the set of integers  $Z_r$ ,  $Z_c \subseteq Z$  and  $H \subseteq Z \times Z$ . For any pair  $(i,j) \in Z \times Z$ , the translate  $H(i,j)$  of  $H$  in the subset  $Z_r \times Z_c$  is defined by:

$$H(i,j) = \{ (m,n) \in Z_r \times Z_c \mid \text{for some } (k,\ell) \in H, \\ m = k + i \text{ and } n = \ell + j \}$$

Figure 2 illustrates a set and some of its translates.

Let  $Z_r \times Z_c$  be the spatial domain of the given binary image  $I$  and  $F$  be that subset of resolution cells in  $Z_r \times Z_c$  which take on the value 1 for image  $I$ .

The erosion  $F \ominus H$  of  $F$  by  $H$  is defined by:

$$F \ominus H = \{(m,n) \in Z \times Z \mid H(m,n) \subseteq F\}$$

The eroded image  $J$  obtained by eroding  $I$  with structural element  $H$  is defined by:

$$J(i,j) = 1 \text{ if and only if } (i,j) \in F \ominus H$$

The number of elements in the erosion  $F \ominus H$  is proportional to the area of the binary 1 figures in the image. An interesting theoretical property of the erosion is that any operation which is anti-extensive, increasing, and idempotent must be made up of erosions (see Matheron<sup>50</sup>, Serra<sup>79</sup>, Lantuejoul<sup>44</sup>).

Textural properties can be obtained from the erosion process by appropriately parametrizing the structural element and determining the number of elements of the erosion as a function of the parameter. For example, in Figure 3 we consider a series of structural elements each of two resolution cells in the same line and separated by distances of 0 through 19. The image in Figure 3 is then eroded by each of these structural elements producing the eroded images of Figure 3. In Figure 4, we illustrate a graph showing the area of the erosion as a function of the distance separating the two resolution cells of the structural elements. A function such as that graphed in Figure 4 is called the covariance function. Notice how it has relative maxima at distances which are multiples of about 5 1/3 resolution cells. This implies that in the horizontal direction there is a strong periodic component in the original image of about 5 1/3 resolution cells.

The generalized covariance function can use more complicated structural elements and summarizes the texture information in the image. If  $H(d)$  is a structural element having two parts where  $d$  represents the distance between these two parts, the generalized covariance function  $k$  for a binary image  $I$  is defined as:

$$k(d) = \#F \ominus H(d), \text{ where } F = \{(i,j) \mid I(i,j) = 1\}$$

For the case where the structural element consists of two resolution cells in the same line separated by distance  $d$ , the generalized covariance reduces to the auto-covariance function for the image  $I$ . The generalized covariance function corresponding to more complicated kinds of structural elements, however, provides information not contained in the auto-covariance function. Serra and Matheron show how the generalized covariance function can determine mean size of tonal features, mean free distance between tonal features, etc.

## II.6 Spatial Gray Tone Dependence: Co-occurrence

One aspect of texture is concerned with the spatial distribution and spatial dependence among the gray tones in a local area. Julesz<sup>39</sup> first used gray tone spatial dependence co-occurrence statistics in texture discrimination experiments. Darling and Joseph<sup>13</sup> used statistics obtained from the nearest neighbor gray tone transition matrix to measure this dependence for satellite images of clouds and was able to identify cloud types on the basis of their texture. Bartels et al.<sup>5</sup> and Weid et al.<sup>93</sup> used one-dimensional co-occurrence in a medical application. Rosenfeld and Troy<sup>77</sup> and Haralick<sup>24</sup> suggested two-dimensional spatial dependence of the gray tones in a co-occurrence matrix for each fixed distance and/or angular spatial

relationship; Haralick et al.<sup>32,33</sup> used statistics of this matrix as measures of texture in satellite imagery (Haralick and Shanmugam<sup>30,31</sup>), aerial, and microscopic imagery (Haralick and Shanmugam<sup>30</sup>). Chien and Fu<sup>10</sup> showed the application of gray tone co-occurrence to automated chest X-ray analysis. Pressman<sup>65</sup> showed the application to cervical cell discrimination. Chen and Pavlidis<sup>9</sup> used co-occurrence in conjunction with a split and merge procedure to segment an image on the basis of texture. All these studies achieved reasonable results on different textures using gray tone co-occurrence.

Suppose the area to be analyzed for texture is rectangular, and has  $N_c$  resolution cells in the horizontal direction,  $N_r$  resolution cells in the vertical direction, and that the gray tone appearing in each resolution cell is quantized to  $N_g$  levels. Let  $L_c = \{1,2,\dots,N_c\}$  be the horizontal spatial domain,  $L_r = \{1,2,\dots,N_r\}$  be the vertical spatial domain, and  $G = \{1,2,\dots,N_g\}$  be the set of  $N_g$  quantized gray tones. The set  $L_r \times L_c$  is the set of resolution cells of the image ordered by their row-column designations. The image  $I$  can be represented as a function which assigns some gray tone in  $G$  to each resolution cell or pair of coordinates in  $L_r \times L_c$ ;  $I: L_r \times L_c \rightarrow G$ .

The gray tone co-occurrence can be specified in a matrix of relative frequencies  $P_{ij}$  with which two neighboring resolution cells separated by distance  $d$  occur on the image, one with gray tone  $i$  and the other with gray tone  $j$ . Such matrices of spatial gray tone dependence frequencies are symmetric and a function of the angular relationship between the neighboring resolution cells as well as a function of the distance between them. For a  $0^\circ$  angular relationship, they explicitly average the probability of a left-right-transition of gray tone  $i$  to gray tone  $j$  within the right-left-transition probability. Figure 5 illustrates the set of all horizontal neighboring resolution cells separated by distance 1. This set, along with the image gray tones, would be used to calculate a distance 1 horizontal spatial gray tone dependence matrix.

Formally, for angles quantized to  $45^\circ$  intervals, the unnormalized frequencies are defined by:

$$P(i,j,d,0^\circ) = \#\{((k,l), (m,n)) \in (L_r \times L_c) \times (L_r \times L_c) \mid k - m = 0, |l - n| = d, I(k,l) = i, I(m,n) = j\}$$

$$P(i,j,d,45^\circ) = \#\{((k,l), (m,n)) \in (L_r \times L_c) \times (L_r \times L_c) \mid (k - m = d, l - n = -d) \text{ or } (k - m = -d, l - n = d), I(k,l) = i, I(m,n) = j\}$$

$$P(i,j,d,90^\circ) = \#\{((k,l), (m,n)) \in (L_r \times L_c) \times (L_r \times L_c) \mid |k - m| = d, l - n = 0, I(k,l) = i, I(m,n) = j\}$$

$$P(i,j,d,135^\circ) = \#\{(k,l), (m,n) \in (L_r \times L_c) \times (L_r \times L_c) \mid (k-m = d, l-n = d) \text{ or } (k-m = -d, l-n = -d), I(k,l) = i, I(m,n) = j\},$$

where # denotes the number of elements in the set.

Note that these matrices are symmetric;  $P(i,j;d,a) = P(j,i;d,a)$ . The distance metric  $\rho$  implicit in the above equations can be explicitly defined by  $\rho((k,l), (m,n)) = \max\{|k-m|, |l-n|\}$ .

Consider Figure 6a, which represents a 4 x 4 image with four gray tones, ranging from 0 to 3. Figure 6b shows the general form of any gray tone spatial dependence matrix. For example, the element in the (2,1)st position of the distance 1 horizontal  $P_H$  matrix is the total number of times two gray tones of values 2 and 1 occurred horizontally adjacent to each other. To determine this number, we count the number of pairs of resolution cells in  $R_H$  such that the first resolution cell of the pair has gray tone 2 and the second resolution cell of the pair has gray tone 1. In Figures 6c through 6f, we calculate all four distance 1 gray tone spatial dependence matrices.

Using features calculated from the co-occurrence matrix (see Figure 7) Haralick et al.<sup>33</sup> performed a number of identification experiments. On a set of aerial imagery and eight terrain classes (old residential, new residential, lake, swamp, marsh, urban, railroad yard, scrub or wooded), an 82 percent correct identification was obtained. On a LANDSAT Monterey Bay, California image, an 84 percent correct identification was obtained using 64 x 64 subimages and both spectral and textural features on seven terrain classes: coastal forest, woodlands, annual grasslands, urban areas, large irrigated fields, small irrigated fields, and water. On a set of sandstone photomicrographs, an 89 percent correct identification was obtained on five sandstone classes: Dexter-L, Dexter-H, St. Peter, Upper Muddy, and Gaskel.

The wide class of images on which they found that spatial gray tone dependence carries much of the texture information is probably indicative of the power and generality of this approach.

The approximate two dozen co-occurrence features times the number of distance angle relationships the co-occurrence matrices can be computed for lead to a potentially large number of dependent features. Tou<sup>88</sup> and Chang<sup>88</sup> discuss an eigenvector-based feature extraction approach to help alleviate this problem.

The experiments of Weszka et al.<sup>92</sup> suggest that the spatial frequency features and, therefore, the autocorrelation feature are not as good measures of texture as the co-occurrence features. We suspect that the reason why co-occurrence probabilities have so much more information than the autocorrelation function is that there tends to be natural constraints between the co-occurrence probabilities at one spatial distance with those at another. By these relationships, a lot of information at one spatial distance can determine the smaller amount of information in the autocorrelation function at many spatial distances.

To illustrate this, consider the one-dimensional conditional co-occurrence probabilities  $\{p_{ij}(\tau)\}$  for

for some specific spatial distance  $\tau$ . Letting  $\mu$  be the mean tone and  $\sigma^2$  be the gray tone variance, and  $p_j$  be the probability of gray tone  $j$  occurring, the autocorrelation function can be written in terms of  $\rho_{ij}$  by

$$\rho(\tau) = \frac{\sum_{i,j} (i-\mu)(j-\mu) p_{ij}(\tau) p_j}{\sigma^2}$$

Hence, for distance  $2\tau$  we have

$$\rho(2\tau) = \frac{\sum_{i,j} (i-\mu)(j-\mu) p_{ij}(2\tau) p_j}{\sigma^2}$$

Assuming the texture is Markov, we have a relationship between  $\{p_{ij}(\tau)\}$  and  $\{p_{ij}(2\tau)\}$ . Namely,

$$p_{ij}(2\tau) = \sum_k p_{ik}(\tau) p_{kj}(\tau)$$

The conditional co-occurrence at one distance can determine the conditional co-occurrence probabilities at another larger distance. Since for any distance, the autocorrelation function is determined by the co-occurrence probabilities, we have that to the extent the texture is Markov, the co-occurrence probabilities at one distance determine the autocorrelation function at many distances.

Because the conditional co-occurrence probabilities are based on a directed distance rather than the undirected distances typically used in the symmetric co-occurrence probabilities, some valuable information may be lost in the symmetric approach. The extent to which such information is lost has not been extensively studied (see Connors and Harlow<sup>11</sup>).

## II.7 A Textural Transform

We wish to construct an image  $J$  such that the gray tone  $J(i,j)$  at resolution cell  $(i,j)$  in image  $J$  indicates how common the texture pattern is in and around resolution cell  $(i,j)$  of image  $I$ . We call the image  $J$  the textural transform of  $I$  (Haralick<sup>25</sup>).

For analysis of the micro-texture, the gray tone  $J(i,j)$  can be a function of the gray tone  $I(i,j)$  and its nearest neighbors.

$$J(i,j) = f(I(i-1,j-1), I(i-1,j), I(i-1,j+1), I(i,j-1), I(i,j), I(i,j+1), I(i+1,j-1), I(i+1,j), I(i+1,j+1))$$

Let us assume that this function  $f$  is an additive effect of horizontal, right diagonal, vertical, and left diagonal relationships. Then

$$J(i,j) = f_1(I(i,j-1), I(i,j), I(i,j+1)) \quad (\text{horizontal}) \\ + f_2(I(i+1,j-1), I(i,j), I(i-1,j+1)) \quad (\text{right diagonal}) \\ + f_3(I(i-1,j), I(i,j), I(i+1,j)) \quad (\text{vertical})$$

$$+ f_4(I(i+1,j+1), I(i,j), I(i-1,j-1))$$

(left diagonal)

But since we do not distinguish between horizontal-left and horizontal-right, or right diagonal up-right and right diagonal down-left, or vertical up and vertical down, or left diagonal up-left and left diagonal down-right, the functions  $f_1$ ,  $f_2$ ,  $f_3$ , and  $f_4$  have additional symmetries. Assuming the spatial relationships between which we do not distinguish contribute additively, we obtain

$$J(i,j) = h_1(I(i,j), I(i,j-1)) + h_1(I(i,j), I(i,j+1)) \quad (\text{horizontal})$$

$$+ h_2(I(i,j), I(i+1,j-1)) + h_2(I(i,j), I(i-1,j+1)) \quad (\text{right diagonal})$$

$$+ h_3(I(i,j), I(i-1,j)) + h_3(I(i,j), I(i+1,j)) \quad (\text{vertical})$$

$$+ h_4(I(i,j), I(i+1,j+1)) + h_4(I(i,j), I(i-1,j-1)) \quad (\text{left diagonal})$$

where the functions  $h_1$ ,  $h_2$ ,  $h_3$ , and  $h_4$  are symmetric functions of two arguments.

Since we want the  $h$  functions to indicate relative frequency of the gray tone spatial pattern, the natural choice is to make each  $h$  the co-occurrence probability corresponding to the horizontal, right diagonal, vertical, or left diagonal spatial relationships.

This concept of textural transform can be generalized to any spatial relationship in the following way.

Let  $Z_r \times Z_c$  be the set of resolution cells of an image  $I$  (by row-column coordinates). Let  $G$  be the set of gray tones possible to appear on image  $I$ . Let  $R$  be a binary relation on  $Z_r \times Z_c$  pairing together all those resolution cells in the desired spatial relation. The co-occurrence matrix  $P$ ,  $P:G \times G \rightarrow [0,1]$ , for image  $I$  and binary relation  $R$  is defined by

$$P(i,j) = \frac{\#\{(a,b),(c,d) \in R \mid I(a,b)=i \text{ and } I(c,d)=j\}}{\#R}$$

The textural transform  $J$ ,  $J:Z_r \times Z_c \rightarrow (-\infty, \infty)$  of image  $I$  relative to function  $f$  is defined by

$$J(r,c) = \frac{1}{\#R(r,c)} \sum_{(a,b) \in R(r,c)} f[P(I(r,c), I(a,b))]$$

Assuming  $f$  to be the identity function, the meaning of  $J(r,c)$  is as follows. The set  $R(r,c)$  is the set of all those resolution cells in  $Z_r \times Z_c$  in the desired spatial relation to resolution cell  $(r,c)$ . For any resolution cell  $(a,b) \in R(r,c)$ ,  $P(I(r,c), I(a,b))$  is the relative frequency by which the gray tone  $I(r,c)$ , appearing at resolution cell  $(r,c)$ , and the gray tone  $I(a,b)$ , appearing at resolution cell  $(a,b)$ , co-occur together in the desired spatial relation on the entire image. The sum

$$\sum_{(a,b) \in R(r,c)} P(I(r,c), I(a,b))$$

is just the sum of the relative frequencies of gray tone co-occurrence over all resolution cells in the specified relation to resolution  $(r,c)$ . The factor  $\frac{1}{\#R(r,c)}$ , the reciprocal of the number of resolution cells in the desired spatial relation to  $(r,c)$ , is just a normalizing factor.

Figure 8 illustrates 27 100 x 100 subimage of band 5 LANDSAT image 1247-15481 laid out according to their proper relationships in the test area. Figure 9 illustrates the textural transforms of these subimages also laid out according to their proper relationships in the test area. Gray tones which are white are indicative of frequently occurring textural patterns in the corresponding area on the original subimage. Gray tones which are black are indicative of infrequently occurring textural patterns in the corresponding area on the original image. This means that the same land use type, depending on how frequently it occurs, can be black or white on the textural transform image.

Examining image (0,0) we notice that Thompson Lake, a U-shaped white area on the lower left side of the subimage and a white area on the right side of the subimage have black tones on the transform image. On image (0,1) Lake Chemung has a large enough area so that its solid black texture appears as a middle gray on the transform image. One image (2,3) Whitmore Lake has a large enough area so that it appears white on the transform image.

We will take a few enlargements of the subimages and their transforms and interpret the textural transform images in terms of the gray tone spatial dependence patterns. Figure 10 shows an enlargement of subimage (1,3) and its transform. Textures consisting of white tones occurring next to white or light gray tones are the most infrequently occurring textural patterns and they appear as black in the transform image. Finally, Figure 11 shows an enlargement of subimage (6,0) where white tones occurring together or black tones occurring together are the most infrequently occurring textural patterns and they appear as black in the transform image.

## II.8 Generalized Gray Tone Spatial Dependence Models for Texture

Given a specific kind of spatial neighborhood (such as a 3 x 2 neighborhood or a 5 x 5 neighborhood) and a subimage it is possible to compute or estimate the joint probability distribution of the gray tone of the neighborhood in the subimage. In the case of a 5 x 5 neighborhood, the joint distribution would be 25-dimensional. The generalized gray tone spatial dependence model for texture is based on this joint distribution. Here, the neighborhood is the primitive, the arrangement of its gray tones is the property, and the texture is characterized by the joint distribution of the gray tones in the neighborhood.

Assuming equal prior probabilities, the probability that any neighborhood belongs to texture class  $k$  is proportional to the probability of the arrangement of the gray tones in the neighborhood as given by the joint distribution for texture class  $k$ . A neighborhood can be assigned to texture class  $k$  if the joint distribution for class  $k$  is maximal.

The problem with the technique is the high dimensionality for the probability distributions. Parametric representation of the distribution by its first

two moments naturally leads to the characterization of texture by the autocorrelation function or power spectrum. Such approaches were discussed in Sections II.2 and II.3. Non-parametric representation of the distribution by histogramming the high-dimensional distributions have sample size and storage problems. In the remainder of this section, we review a discrimination technique for representing the non-zero support for these distributions.

Histogram approaches to representing the neighborhood distribution function must pay a heavy storage penalty. For example, a 3 x 3 neighborhood with 4 quantized values for each gray tone requires  $4^9$  storage locations (over 250,000). To handle this problem, Read and Jayaramamurthy<sup>67</sup> and McCormick and Jayaramamurthy<sup>54</sup> suggest using the set covering methodology of Michalski<sup>54</sup> and Michalski and McCormick<sup>55</sup> to keep track of those histogram bins which would be non-empty. This technique allows for the generalization of the observed texture samples for each class and provides a simple table look-up sort of decision rule (Haralick<sup>26</sup>).

To see how this works, let the given type of neighborhood contain N resolution cells and let G be the set of quantized gray tones. Then  $G^N$  is the set of all possible arrangements of gray tones in the neighborhood. Let  $S_k \subseteq G^N$  be the training set of all observed neighborhoods of texture k,  $k = 1, \dots, K$ . We will assume that  $S_k \cap S_m = \emptyset$  for  $k \neq m$ .

To generalize the training sets, we employ a cylinder operator (Haralick<sup>27</sup>). Let J be a subset of the indexes from 1 to N;  $J \subseteq \{1, \dots, N\}$ . The cylinder operator  $\Psi_J$  operates on N-tuples of  $G^N$  constraining all components indexed by J to remain fixed to the values they currently hold and letting go free the values for all components not indexed by J. In this manner, under the  $\Psi_{\{2, \dots, N\}}$  operator, the N-tuple  $(x_1, \dots, x_N)$  becomes  $(*, x_2, \dots, x_N)$  where \* means any value. Formally, for any  $A \subseteq G^N$ , we define the order #J cylinder operator  $\Psi_J$  by:

$$\Psi_J(A) = \{(g_1, \dots, g_N) \in G^N \mid \text{for some } (a_1, \dots, a_N) \in A, \\ g_j = a_j \text{ for all } j \in J\}$$

The cylinder operator is used to generalize the samples of observed texture from each texture class by creating a minimal cover of that class against all other classes. A cover for class k is a collection of subsets of  $G^N$  each of which has non-empty intersection with  $S_k$  and empty intersection with  $S_m$ ,  $m \neq k$ . An

order-M cover of  $S_k$  against  $\bigcup_{\substack{m=1 \\ m \neq k}}^K S_m$  is a collection

$\mathcal{L}_k^M$  of subsets of  $G^N$ , each subset in the collection generalizing an N-tuple in  $S_k$  by an order-M or less cylinder operator.

$$\mathcal{L}_k^M = \{A \subseteq G^N \mid \text{for some } (x_1, \dots, x_N) \in S_k \text{ and} \\ \text{index set } J, \#J \leq M, A = \Psi_J(x_1, \dots, x_N) \text{ and} \\ A \cap S_m = \emptyset, m \neq k\}$$

It is clear that when the observed sample sets  $S_k$  are disjoint, it is always possible to find a cover of  $S_k$  since we can take the order  $M = N$  making  $\mathcal{L}_k^N$  contain precisely the singleton sets whose members are elements of  $S_k$ . Hence, for large enough M, it is always possible to make  $\mathcal{L}_k^M$  satisfy:

$$S_k \subseteq \bigcup_{A \in \mathcal{L}_k^M} A \quad A \subseteq \left( \bigcup_{\substack{\ell=1 \\ \ell \neq k}}^K S_\ell \right)^c \quad (1)$$

We will call an order-M cover minimal if by using cylinder operators only of order less than M, equation (1) cannot be satisfied.

The labeling of neighborhoods by texture class can proceed in the following way. Let  $\mathcal{L}_1, \dots, \mathcal{L}_K$  be minimal covers. Let  $(g_1, \dots, g_N)$  be an N-tuple of gray tones from a neighborhood. If the N-tuple is in the cover for class k and for no other class, then assign it to class k. Hence, if:

$$(1) (g_1, \dots, g_N) \in \bigcup_{A \in \mathcal{L}_k} A \text{ and}$$

$$(2) (g_1, \dots, g_N) \notin \bigcup_{A \in \mathcal{L}_m} A, m \neq k,$$

then we assign the neighborhood to texture class k. If there exists no class so that (1) and (2) are simultaneously satisfied, then we reserve decision.

Using a decision rule similar to this but with a definition for cover minimality which makes the cover dependent on the order in which the N-tuples are encountered, Read and Jayaramamurthy<sup>67</sup> achieved a 78 percent correct identification in distinguishing two textures of chromatin samples and artifact samples from pap smears using a 3 x 2 neighborhood and a 4 gray level quantization.

## II.9 Run Lengths

A gray level run length primitive is a maximal collinear connected set of pixels all having the same gray tone. Gray level runs can be characterized by the gray tone of the run, the length of the run, and the direction of the run. Galloway<sup>21</sup> used 4 directions:  $0^\circ$ ,  $45^\circ$ ,  $90^\circ$ , and  $135^\circ$ , and for each of these directions she computed the joint probability of gray tone of run and run length.

Let  $p(i, j)$  be the number of times there is a run length j and having gray tone i. Let  $N_g$  be the number of gray tones and  $N_r$  be the number of runs. Useful statistics of the  $p(i, j)$  include:

$$\sum_{i=1}^{N_g} \sum_{j=1}^{N_r} \frac{p(i, j)}{j^2} / \sum_{i=1}^{N_g} \sum_{j=1}^{N_r} p(i, j) \quad (\text{short run} \\ \text{emphasis} \\ \text{inverse moments})$$

$$\sum_{i=1}^{N_g} \sum_{j=1}^{N_r} j^2 p(i, j) / \sum_{i=1}^{N_g} \sum_{j=1}^{N_r} p(i, j) \quad (\text{long run} \\ \text{emphasis} \\ \text{moments})$$



$$\frac{\sum_{i=1}^{N_g} \left( \sum_{j=1}^{N_r} p(i,j) \right)^2}{\sum_{i=1}^{N_g} \sum_{j=1}^{N_r} p(i,j)} \quad (\text{gray level non-uniformity})$$

$$\frac{\sum_{j=1}^{N_r} \left( \sum_{i=1}^{N_g} p(i,j) \right)^2}{\sum_{i=1}^{N_g} \sum_{j=1}^{N_r} p(i,j)} \quad (\text{run length non-uniformity})$$

$$\frac{\sum_{i=1}^{N_g} \sum_{j=1}^{N_r} p(i,j)}{\sum_{i=1}^{N_g} \sum_{j=1}^{N_r} j p(i,j)} \quad (\text{fraction of image in runs})$$

Using these five measures for each of 4 directions and one of Haralick's data sets, Galloway illustrated that about 83 percent identification could be made of the six categories: swamp, lake, railroad, orchard, scrub, and suburb.

## II.10 Auto-Regression Models

The linear dependence one pixel of an image has on another is well known and can be illustrated by the autocorrelation function. This linear dependence is exploited by the auto-regression model for texture

which was first used by McCormick and Jayarammurthy<sup>52</sup> to synthesize textures. McCormick and Jayarammurthy used the Box and Jenkins<sup>6</sup> time series seasonal analysis method to estimate the parameters of a given texture. They then used the estimated parameters and a given set of starting values to illustrate that the synthesized texture was close in appearance to the given texture. Deguchi and Morishita<sup>15</sup>, Tou et al.<sup>89</sup>, and Tou and Chang<sup>87</sup> also use a similar technique.

Figure 12 shows this texture synthesis model. Given a randomly generated noise image and any sequence of K synthesized gray tone values in a scan, the next gray tone value can be synthesized as a linear combination of the previously synthesized values plus a linear combination of previous L random noise values. The coefficients of these linear combinations are the parameters of the model.

Although the one-dimensional model employed by Read and Jayarammurthy worked reasonably well for the two vertical streaky textures on which they illustrated the technique, performance would be poorer on diagonal wiggly streaky textures. Better performance on general textures would be achieved by a full two-dimensional model in Figure 13. Here a pixel (i,j) depends on a two-dimensional neighborhood N(i,j) consisting of pixels above or to the left of it as opposed to the simple sequence of the previous pixels a raster scan could define. For each pixel (k,l) in an order-D neighborhood for pixel (i,j), (k,l) must be previous to pixel (i,j) in a standard raster sequence and (k,l) must not have any coordinates more than D units away from (i,j). Formally, the order-D neighborhood is defined by:

$$N(i,j) = \{(k,l) \mid (i-D \leq k < i \text{ and } j-D \leq l \leq j+D) \text{ or } (k=i \text{ and } j-D \leq l < j)\}$$

The auto-regressive model can be employed in texture segmentation applications as well as texture synthesis applications. Let  $\{\alpha_c(m,n), \beta_c(m,n)\}$  be the coefficients for texture category c and let  $\theta$  be a threshold value. Define the estimated value of the gray tone at resolution cell (i,j) by:

$$\hat{a}_c(i,j) = \sum_{(k,l) \in N(i,j)} a_c(i-k, j-l) a_c(k,l) +$$

$$\sum_{(k,l) \in N(i,j)} \beta_c(i-k, j-l) [a_c(k,l) - \hat{a}_c(k,l)]$$

See Figure 14.

Assuming a uniform prior distribution, we can decide pixel (i,j) has texture category k if:

$$|a(i,j) - \hat{a}_k(i,j)| \leq |a(i,j) - \hat{a}_l(i,j)| \text{ for every } l \text{ and } |a(i,j) - \hat{a}_k(i,j)| \leq \theta$$

If  $|a(i,j) - \hat{a}_k(i,j)| > \theta$ , then decide pixel (i,j) is a boundary pixel.

Those readers interested in general two-dimensional estimation procedures for images will find Woods<sup>94</sup> of interest.

## III. STRUCTURAL APPROACHES TO TEXTURE MODELS

Pure structural models of texture are based on the view that textures are made up of primitives which appear in near regular repetitive spatial arrangements. To describe the texture, we must describe the primitives and the placement rules (Rosenfeld and Lipkin<sup>73</sup>). The choice of which primitive from a set of primitives and the probability of the chosen primitive being placed at a particular location can be a strong or weak function of location or the primitives near the location.

Carlucci<sup>8</sup> suggests a texture model using primitives of line segments, open polygons, and closed polygons in which the placement rules are given syntactically in a graph-like language. Zucker<sup>98</sup> conceives of real texture as being a distortion of an ideal texture. The underlying ideal texture has a nice representation as a regular graph in which each node is connected to its neighbors in an identical fashion. Each node corresponds to a cell in a tessellation of the plane. The underlying ideal texture is transformed by distorting the primitive at each node to make a realistic texture. Zucker's model is more of a competence based model than a performance model.

Lu and Fu<sup>47</sup> give a tree grammar syntactic approach for texture. They divide a texture up into small square windows (9 x 9). The spatial structure of the resolution cells in the window is expressed as a tree. The assignment of gray tones to the resolution is given by the rules of a stochastic tree grammar. Finally, special case is given to the placement of windows with respect to another in order to preserve the coherence between windows. Lu and Fu illustrate the power of their technique with both texture synthesis and texture experiments.

In the remainder of this section, we discuss some structural-statistical approaches to texture models. The approach is structural in the sense that primitives are explicitly defined. The approach is statistical in that the spatial interaction, or lack of it, between primitives is measured by probabilities.

We classify textures as being weak textures, or strong textures. Weak textures are those which have weak spatial-interaction between primitives. To distinguish between them it may be sufficient to only determine the frequency with which the variety of primitive kinds occur in some local neighborhood. Hence, weak texture measures account for many of the statistical textural features. Strong textures are those which have non-random spatial interactions. To distinguish them it may be sufficient to only determine, for each pair of primitives, the frequency with which the primitives co-occur in a specified spatial relationship. Thus, our discussion will center on the variety of ways in which primitives can be defined and the ways in which spatial relationships between primitives can be defined.

### III.1 Primitives

A primitive is a connected set of resolution cells characterized by a list of attributes. The simplest primitive is the pixel with its gray tone attribute. Sometimes it is useful to work with primitives which are maximally connected sets of resolution cells having a particular property. An example of such a primitive is a maximally connected set of pixels all having the same gray tone or all having the same edge direction.

Gray tones and local properties are not the only attributes which primitives may have. Other attributes include measures of shape of connected region and homogeneity of its local property. For example, a connected set of resolution cells can be associated with its length or elongation of its shape or the variance of its local property.

Many kinds of primitives can be generated or constructed from image data by simple 3 x 3 neighborhood operators. Included in this class of primitives are:

1. Connected components
2. Ascending or descending components
3. Saddle components
4. Relative maxima or minima components
5. Central axis components

Neighborhood operators which compute these kinds of primitives can be found in a variety of papers and will not be discussed here. See Rosenfeld and Pfaltz<sup>74</sup>; Rosenfeld<sup>68</sup>; Rosenfeld<sup>69</sup>; Rosenfeld<sup>70</sup>; Rosenfeld and Davis<sup>71</sup>; Yokoi, Toriwaki, and Fukumura<sup>94</sup>; Arcelli and Sanniti di Baja<sup>1</sup>; and Haralick<sup>27</sup>.

### III.2 Spatial Relationships

Once the primitives have been constructed, we have available a list of primitives, their center coordinates, and their attributes. We might also have available some topological information about the primitives, such as which are adjacent to which. From this data, we can select a simple spatial relationship such as adjacency of primitives or nearness of primitives and count how many primitives of each kind occur in the specified spatial relationship.

More complex spatial relationships include closest distance or closest distance within an angular window. In this case, for each kind of primitive situated in the texture, we could lay expanding circles around it and locate the shortest distance between it and every other kind of primitive. In this case our co-occurrence frequency is three-dimensional, two dimensions for primitive kind and one dimension for shortest distance. This can be dimensionally reduced to two dimensions by

considering only the shortest distance between each pair of like primitives.

### III.3 Weak Texture Measures

Tsuji and Tomita<sup>91</sup> and Tomita, Yachida, and Tsuji<sup>85</sup> describe a structural approach to weak texture measures. First a scene is segmented into atomic regions based on some tonal property such as constant gray tone. These regions are the primitives. Associated with each primitive is a list of properties such as size and shape. Then they make a histogram of size property or shape property over all primitives in the scene. If the scene can be decomposed into two or more regions of homogeneous texture, the histogram will be multi-modal. If this is the case, each primitive in the scene can be tagged with the mode in the histogram it belongs to. A region growing/cleaning process on the tagged primitives yields the homogeneous textural region segmentation.

If the initial histogram modes overlap too much, a complete segmentation may not result. In this case, the entire process can be repeated with each of the then so far found homogeneous texture region segments. If each of the homogeneous texture regions consists of mixtures of more than one type of primitive, then the procedure may not work at all. In this case, the technique of co-occurrence of primitive properties would have to be used.

Zucker et al.<sup>99</sup> used a form of this technique by filtering a scene with a spot detector. Non-maxima pixels in the filtered scene were thrown out. If a scene has many different homogeneous texture regions, the histogram of the relative max spot detector filtered scene will be multi-modal. Tagging the maxima with the modes they belong to and region growing/cleaning thus produced the segmented scene.

The idea of the constant gray level regions of Tsuji and Tomita or the spots of Zucker et al. can be generalized to regions which are peaks, pits, ridges, ravines, hillsides, passes, breaks, flats, and slopes. (Toriwaki and Fukumura<sup>86</sup>, Peucker and Douglas<sup>63</sup>). In fact, the possibilities are numerous enough that investigators doing experiments will have a long working period before understanding will exhaust the possibilities. The next three subsections review in greater detail some specific approaches and suggest some generalizations.

#### III.3.1 Edge Per Unit Area

Rosenfeld and Troy<sup>77</sup> and Rosenfeld and Thurston<sup>76</sup> suggested the amount of edge per unit area for a texture measure. The primitive here is the pixel and its property is the magnitude of its gradient. The gradient can be calculated by any one of the gradient neighborhood operators. For some specified window centered on a given pixel, the distribution of gradient magnitudes can then be determined. The mean of this distribution is the amount of edge per unit area associated with the given pixel. The image in which each pixel's value is edge per unit area is actually a defocussed gradient image. Triendl<sup>90</sup> used a defocussed Laplacian image. Sutton and Hall<sup>83</sup> used such a measure for the automatic classification of pulmonary disease in chest X-rays.

Ohlander<sup>60</sup> used such a measure to aid him in segmenting textured scenes. Rosenfeld<sup>70</sup> gives an example where the computation of gradient direction on a defocussed gradient image is an appropriate feature for

the direction of texture gradient. Hsu<sup>38</sup> used a variety of gradient-like measures.

### III.3.2 Run Lengths

The gray level run lengths primitive in its one-dimensional form is a maximal collinear connected set of pixels all having the same gray level. Properties of the primitive can be length of run, gray level, and angular orientation of run. Statistics of these properties were used by Galloway<sup>21</sup> to distinguish between textures.

In the two-dimensional form, the gray level run length primitive is a maximal connected set of pixels all having the same gray level. These maximal homogeneous sets have properties such as number of pixels, maximum or minimum diameter, gray level, angular orientation of maximum or minimum diameter.

### III.3.3 Relative Extrema Density

Rosenfeld and Troy<sup>77</sup> suggest the number of extrema per unit area for a texture measure. They suggest defining extrema in one-dimension only along a horizontal scan in the following way: in any row of pixels a pixel  $i$  is a relative minimum if its gray tone  $g(i)$  satisfies:

$$g(i) \leq g(i+1) \text{ and } g(i) \leq g(i-1) \quad (1)$$

A pixel  $i$  is a relative maximum if:

$$g(i) \geq g(i+1) \text{ and } g(i) \geq g(i-1) \quad (2)$$

Note that with this definition each pixel in the interior of any constant gray tone run of pixels is considered simultaneously a relative minimum and relative maximum. This is so even if the constant run is just a plateau on the way down or on the way up from a relative extrema.

The algorithm employed by Rosenfeld and Troy marks every pixel in each row which satisfies equations (1) or (2). Then they center a square window around each pixel and count the number of marked pixels. The texture image created this way corresponds to a defocused marked image.

Mitchell, Myers, and Boyne<sup>56</sup> suggest the extrema idea of Rosenfeld and Troy except they proposed to use true extrema and to operate on a smoothed image to eliminate extrema due to noise. See also Carlton and Mitchell<sup>7</sup>, and Ehrich and Foith<sup>18,19</sup>.

One problem with simply counting all extrema in the same extrema plateau as extrema is that extrema per unit area is not sensitive to the difference between a region having few large plateaus of extrema and many single pixel extrema. The solution to this problem is to only count an extrema plateau once. This can be achieved by locating some central pixel in the extrema plateau and marking it as the extrema associated with the plateau. Another way of achieving this is to associate a value of  $1/N$  for every extrema in a  $N$ -pixel extrema plateau.

In the one-dimensional case, there are two properties that can be associated with every extrema: its height and its width. The height of a maxima can be defined as the difference between the value of the maxima and the highest adjacent minima. The height (depth) of a minima can be defined as the difference between the value of the minima and the lowest adjacent maxima. The width of a maxima is the distance

between its two adjacent minima. The width of a minima is the distance between its two adjacent maxima. Figure 15 illustrates these properties.

Two-dimensional extrema are more complicated than one-dimensional extrema. One way of finding extrema in the full two-dimensional sense is by the iterated use of some recursive neighborhood operators propagating extrema values in an appropriate way. Maximally connected areas of relative extrema may be areas of single pixels or may be plateaus of many pixels. We can mark each pixel in a relative extrema region of size  $N$  with the value  $h$  indicating that it is part of a relative extrema having height  $h$  or mark it with the value  $h/N$  indicating its contribution to the relative extrema area. Alternatively, we can mark the most centrally located pixel in the relative extrema region with the value  $h$ . Pixels not marked can be given the value 0. Then for any specified window centered on a given pixel, we can add up the values of all pixels in the window. This sum divided by the window size is the average height of extrema in the area. Alternatively we could set  $h$  to 1 and the sum would be the number of relative extrema per unit area to be associated with the given pixel.

Going beyond the simple counting of relative extrema, we can associate properties to each relative extrema. For example, given a relative extrema, we can determine the set of all pixels reachable only by the given relative maxima and not by any other relative maxima by monotonically decreasing paths. This set of reachable pixels is a connected region and forms a mountain. Its border pixels may be relative minima or saddle pixels.

The relative height of the mountain is the difference between its relative maxima and the highest of its exterior border pixels. Its size is the number of pixels which constitute it. Its shape can be characterized by features such as elongation, circularity, and symmetric axis. Elongation can be defined as the ratio of the larger to small eigenvalue of the  $2 \times 2$  second moment matrix obtained from the  $\begin{pmatrix} x \\ y \end{pmatrix}$  coordinates of the border pixels (Bachi<sup>2</sup>, Frolov<sup>20</sup>). Circularity can be defined as the ratio of the standard deviation to the mean of the radii from the region's center to its border (Haralick<sup>25</sup>). The symmetric axis feature can be determined by thinning the region down to its skeleton and counting the number of pixels in the skeleton. For regions which are elongated, it may be important to measure the direction of the elongation or the direction of the symmetric axis.

Osman and Saukar<sup>62</sup> use the mean and variance of the height of mountain or depth of valley as properties of primitives. Tsuji and Tomita<sup>91</sup> use size. Histograms and statistics of histograms of these primitive properties are all suitable measures for weak textures.

### III.3.4 Relational Trees

Ehrich and Foith<sup>18</sup> describe a relational tree representation for the extrema of one-dimensional functions with bounded domains. The relational tree recursively partitions the function and its domain at the smallest relative minimum. The relative minimums for the newly formed segments and functions to the left and right of the dividing point can be used for further divisions. An alternative way to form the tree is to use maximums instead of minimums for dividing.

Figure 16 illustrates a function and Figure 17 illustrates its relational tree. The root of the tree indicates that over the entire function domain the highest relative maximum is point 16 and the lowest relative minimum is point 23. The function is then divided at valley 23. The segment to the right of 23 has point 26 for the highest relative maximum and point 27 for the lowest relative minimum, and so on.

Textural features can be extracted at any level of the relational tree. One such texture feature is segment contrast. Segment contrast is the difference between the largest relative maximum and the smallest relative minimum in the segment. The segment contrast textural feature can be the mean or variance of segment contrast taken over the set of segments comprising the given function at a specified level of the tree. Another textural feature can be the variance of segment length.

### III.4 Strong Texture Measures and Generalized Co-occurrence

Strong texture measures take into account the co-occurrence between texture primitives. On the basis of Julesz<sup>46</sup> it is probably the case that the most important interaction between texture primitives occurs as a two-way interaction. Textures with identical second and lower order interactions but with different higher order interactions tend to be visually similar.

The simplest texture primitive is the pixel with its gray tone property. Gray tone co-occurrence between neighboring pixels was suggested as a measure of texture by a number of researchers as discussed in Section II.6. All the studies mentioned there achieved a reasonable classification accuracy of different textures using co-occurrences of the gray tone primitive.

The next more complicated primitive is a connected set of pixels homogeneous in tone. (Tsuji and Tomita<sup>91</sup>). Such a primitive can be characterized by size, elongation, orientation, and average gray tone. Useful texture measures include co-occurrence of primitives based on relationships of distance or adjacency. Maleson et al.<sup>48</sup> suggests using region growing techniques and ellipsoidal approximations to define the homogeneous regions and degree of co-linearity as one basis of co-occurrence. For example, for all primitives of elongation greater than a specified threshold we can use the angular orientation of each primitive with respect to its closest neighboring primitive as a strong measure of texture.

Relative extrema primitives were proposed by Rosenfeld and Troy<sup>77</sup>; Mitchell, Myers, and Boyne<sup>56</sup>; Ehrich and Foith<sup>18</sup>; Mitchell and Carlton<sup>57</sup>; and Ehrich and Foith<sup>19</sup>. Co-occurrence between relative extrema was suggested by Davis et al.<sup>14</sup>. Because of their invariance under any monotonic gray scale transformation, relative extrema primitives are likely to be very important.

It is possible to segment an image on the basis of relative extrema (for example, relative maxima) in the following way: label all pixels in each maximally connected relative maxima plateau with a unique label. Then label each pixel with the label of the relative maxima that can reach it by a monotonically decreasing path. If more than one relative maxima can reach it by a monotonically decreasing path, then label the

pixel with a special label "c" for common. We call the regions so formed the descending components of the image.

Co-occurrence between properties of the descending components can be based on the spatial relationship of adjacency. For example, if the property is size, the co-occurrence matrix could tell us how often a descending component of size  $s_1$  occurs adjacent to or nearby to a descending component of size  $s_2$  or of label "c".

To define the concept of generalized co-occurrence it is necessary to first decompose an image into its primitives. Let  $Q$  be the set of all primitives on the image. Then we need to measure primitive properties such as mean gray tone, variance of gray tones, region, size, shape, etc. Let  $T$  be the set of primitive properties and  $f$  be a function assigning to each primitive in  $Q$  a property of  $T$ . Finally, we need to specify a spatial relation between primitives such as distance or adjacency. Let  $S \subseteq Q \times Q$  be the binary relation pairing all primitives which satisfy the spatial relation. The generalized co-occurrence matrix  $P$  is defined by:

$$P(t_1, t_2) = \frac{\#\{(q_1, q_2) \in S \mid f(q_1) = t_1 \text{ and } f(q_2) = t_2\}}{\#S}$$

$P(t_1, t_2)$  is just the relative frequency with which two primitives occur with specified spatial relationship in the image, one primitive having property  $t_1$  and the other primitive having property  $t_2$ .

Zucker<sup>97</sup> suggests that some textures may be characterized by the frequency distribution of the number of primitives any primitive has related to it. This probability  $p(k)$  is defined by:

$$p(k) = \frac{\#\{(q \in Q \mid \#S(q) = k\}}{\#Q}$$

Although this distribution is simpler than co-occurrence, no investigator appears to have used it in texture discrimination experiments.

## IV. CONCLUSION

We have surveyed the image processing literature on the various approaches and models investigators have used for textures. For micro-textures, the statistical approach seems to work well. The statistical approaches have included autocorrelation functions, optical transforms, digital transforms, textural edgeness, structural element, gray tone co-occurrence, and auto-regressive models. Pure structural approaches based on more complex primitives than gray tone seems not to be widely used. For macro-textures, investigators seem to be moving in the direction of using histograms of primitive properties and co-occurrence of primitive properties in a structural-statistical generalization of the pure structural and statistical approaches.

## REFERENCES

1. Arcelli, Carlo and Gabriella Sanniti Di Baja, "On the Sequential Approach to Medial Line Transformation," *IEEE Transactions on Systems, Man, and Cybernetics*, Vol. SMC-8, No. 2, February 1978, pp. 139-144.

2. Bachi, Roberto, "Geostatistical Analysis of Territories," Proceedings of the 39th Session -- Bulletin of the International Statistical Institute, Vienna, 1973.
3. Bajcsy, R. and L. Lieberman, "Computer Description of Real Outdoor Scenes," Proceedings of Second International Joint Conference on Pattern Recognition, Copenhagen, Denmark, August 1974, pp. 174-179.
4. Bajcsy, R. and L. Lieberman, "Texture Gradient as a Depth Cue," Computer Graphics and Image Processing, Vol. 5, No. 1, 1976, pp. 52-67.
5. Bartels, P., G. Bahr, and G. Weid, "Cell Recognition from Line Scan Transition Probability Profiles," Acta Cytol., Vol. 13, 1969, pp. 210-217.
6. Box, J.E. and G.M. Jenkins, Time Series Analysis, Holden-Day, San Francisco, California, 1970.
7. Carlton, S.G. and O. Mitchell, "Image Segmentation Using Texture and Grey Level," Pattern Recognition and Image Processing Conference, Troy, New York, June 1977, pp. 387-391.
8. Carlucci, L., "A Formal System for Texture Languages," Pattern Recognition, Vol. 4, 1972, pp. 53-72.
9. Chen, P. and T. Pavlidis, "Segmentation by Texture Using a Co-occurrence Matrix and a Split-and-Merge Algorithm," Technical Report 237, Princeton University, Princeton, New Jersey, January 1978.
10. Chien, Y.P. and K.S. Fu, "Recognition of X-Ray Picture Patterns," IEEE Transactions on Systems, Man, and Cybernetics, Vol. SMC-4, No. 2, March 1974, pp. 145-156.
11. Connors, Richard W. and Charles A. Harlow, "Some Theoretical Considerations Concerning Texture Analysis of Radiographic Images," Proceedings of the 1976 IEEE Conference on Decision and Control, 1976.
12. Cutrona, L.J., E.N. Leith, C.J. Palermo, and L.J. Porcello, "Optical Data Processing and Filtering Systems," IRE Transactions on Information Theory, Vol. 15, No. 6, June 1969, pp. 386-400.
13. Darling, E.M. and R.D. Joseph, "Pattern Recognition from Satellite Altitudes," IEEE Transactions on Systems, Man, and Cybernetics, Vol. SMC-4, March 1968, pp. 38-47.
14. Davis, L., S. Johns, and J.K. Aggarwal, "Texture Analysis Using Generalized Co-occurrence Matrices," Pattern Recognition and Image Processing Conference, Chicago, Illinois, May 31 - June 2, 1978.
15. Deguchi, K. and I. Morishita, "Texture Characterization and Texture-Based Image Partitioning Using Two-Dimensional Linear Estimation Techniques," U.S. - Japan Cooperative Science Program Seminar on Image Processing in Remote Sensing, Washington, DC, November 1-5, 1976.
16. Dyer, C. and A. Rosenfeld, "Fourier Texture Features: Suppression of Aperture Effects," IEEE Transactions on Systems, Man, and Cybernetics, Vol. SMC-6, No. 10, October 1976, pp. 703-705.
17. Egbert, D., J. McCauley, and J. McNaughton, "Ground Pattern Analysis in the Great Plains," Semi-Annual ERTS A Investigation Report, Remote Sensing Laboratory, University of Kansas, Lawrence, Kansas, August 1973.
18. Ehrich, Roger and J.P. Foith, "Representation of Random Waveforms by Relational Trees," IEEE Transactions on Computers, Vol. C-25, No. 7, July 1976, pp. 725-736.
19. Ehrich, Roger and J.P. Foith, "Topology and Semantics of Intensity Arrays," Computer Vision, Hanson and Riseman (Editors), Academic Press, New York, 1978.
20. Frolov, Y.S., "Measuring the Shape of Geographical Phenomena: A History of the Issue," Soviet Geography: Review and Translation, Vol. XVI, No. 10, December 1975, pp. 676-687.
21. Galloway, M., "Texture Analysis Using Gray Level Run Lengths," Computer Graphics and Image Processing, Vol. 4, 1974, pp. 172-199.
22. Goodman, J.W., Introduction to Fourier Optics, McGraw-Hill Book Company, New York, 1968.
23. Gramenopoulos, Nicholas, "Terrain Type Recognition Using ERTS-1 MSS Images," Symposium on Significant Results Obtained from the Earth Resources Technology Satellite, NASA SP-327, March 1973, pp. 1229-1241.
24. Haralick, R.M., "A Texture-Context Feature Extraction Algorithm for Remotely Sensed Imagery," Proceedings of the 1971 IEEE Decision and Control Conference, Gainesville, Florida, December 15-17, 1971, pp. 650-657.
25. Haralick, R.M., "A Textural Transform for Images," Proceedings of the IEEE Conference on Computer Graphics, Pattern Recognition, and Data Structure, Beverly Hills, California, May 14-16, 1975.
26. Haralick, R.M., "The Table Look-Up Rule," Communications in Statistics--Theory and Methods, Vol. A5, No. 12, 1976, pp. 1163-1191.
27. Haralick, R.M., "Structural Pattern Recognition, Homomorphisms, and Arrangements," Pattern Recognition, Vol. 10, No. 3, June 1978.
28. Haralick, R.M. and R. Bosley, "Texture Features for Image Classification," Third ERTS Symposium, NASA SP-351, NASA Goddard Space Flight Center, Greenbelt, Maryland, December 10-15, 1973, pp. 1929-1969.
29. Haralick, R.M. and K. Shanmugam, "Combined Spectral and Spatial Processing of ERTS Imagery Data," Second Symposium on Significant Results Obtained from Earth Resources Technology Satellite - 1, NASA SP-327, NASA Goddard Space Flight Center, Greenbelt, Maryland, March 5-9, 1973, pp. 1219-1228.
30. Haralick, R.M. and K. Shanmugam, "Computer Classification of Reservoir Sandstones," IEEE Transactions on Geoscience Electronics, Vol. GE-11, No. 4, October 1973, pp. 171-177.

31. Haralick, R.M. and K. Shanmugam, "Combined Spectral and Spatial Processing of ERTS Imagery Data," Journal of Remote Sensing of the Environment, Vol. 3, 1974, pp. 3-13.
32. Haralick, R.M., K. Shanmugam, and I. Dinstein, "On Some Quickly Computable Features for Texture," Proceedings of the 1972 Symposium on Computer Image Processing and Recognition, University of Missouri, Vol. 2, August 1972, pp. 12-2-1 to 12-2-10.
33. Haralick, R.M., K. Shanmugam, and I. Dinstein, "Textural Features for Image Classification," IEEE Transactions on Systems, Man, and Cybernetics, Vol. SMC-3, No. 6, November 1973, pp. 610-621.
34. Haralick, R.M., "Neighborhood Operators," unpublished manuscript.
35. Hardy, E.E. and J.R. Anderson, "A Land Use Classification System for Use with Remote-Sensor Data," Machine Processing of Remotely Sensed Data, Lafayette, Indiana, October 1973.
36. Hawkins, Joseph K., "Textural Properties for Pattern Recognition," Picture Processing and Psychopictorics, Bernic Sacks Lipkin and Azriel Rosenfeld (Editors), Academic Press, New York, 1969.
37. Horning, R.J. and J.A. Smith, "Application of Fourier Analysis to Multi-spectral/Spatial Recognition," Management and Utilization of Remote Sensing Data ASP Symposium, Sioux Falls, South Dakota, October 1973.
38. Hsu, S., "A Texture-Tone Analysis for Automated Landuse Mapping with Panchromatic Images," Proceedings of the American Society for Photogrammetry, March 1977, pp. 203-215.
39. Julesz, Bela, "Visual Pattern Discrimination," IRE Transactions on Information Theory, Vol. 8, No. 2, February 1962, pp. 84-92.
40. Julesz, Bela, "Experiments in the Visual Perception of Texture," April 1975, 10 pages.
41. Kaizer, H., "A Quantification of Textures on Aerial Photographs," Boston University Research Laboratories, Technical Note 121, 1955, AD 69484.
42. Kirvida, L., "Texture Measurements for the Automatic Classification of Imagery," IEEE Transactions on Electromagnetic Compatibility, Vol. 18, No. 1, February 1976, pp. 38-42.
43. Kirvida, L. and G. Johnson, "Automatic Interpretation of ERTS Data for Forest Management," Symposium on Significant Results Obtained from the Earth Resources Technology Satellite, NASA SP-327, March 1973.
44. Lanteujoul, C., "Grain Dependence Test in a Polycrystalline Ceramic," Quantitative Analysis of Microstructures in Materials Science, Biology, and Medicine, J.L. Chernant (Editor), Dr. Riederer-Verlag, GmbH, Stuttgart, 1978, pp. 40-50.
45. Lendaris, G. and G. Stanley, "Diffraction Pattern Sampling for Automatic Pattern Recognition," SPIE Pattern Recognition Studies Seminar Proceedings, June 9-10, 1969, pp. 127-154.
47. Lu, S.Y. and K.S. Fu, "A Syntactic Approach to Texture Analysis," Computer Graphics and Image Processing, Vol. 7, 1978, pp. 303-330.
48. Maleson, Joseph, C. Brown, and J. Feldman, "Understanding Natural Texture," Computer Science Department, University of Rochester, Rochester, New York, September 1977.
49. Matheron, G., Elements Pour Une Theorie des Milieux Poreux, Masson, Paris, 1967.
50. Matheron, G., Random Sets and Integral Geometry, Wiley and Sons, Inc., New York, 1975.
51. Maurer, H., "Texture Analysis with Fourier Series," Proceedings of the Ninth International Symposium on Remote Sensing of Environment, Environmental Research Institute of Michigan, Ann Arbor, Michigan, April 1974, pp. 1411-1420.
52. McCormick, B.H. and S.N. Jayaramamurthy, "Time Series Model for Texture Synthesis," International Journal of Computer and Information Sciences, Vol. 3, No. 4, December 1974, pp. 329-343.
53. McCormick, B.H. and S.N. Jayaramamurthy, "A Decision Theory Method for the Analysis of Texture," International Journal of Computer and Information Sciences, Vol. 4, No. 1, March 1975, pp. 1-38.
54. Michalski, R.S., "On the Quasi-Minimal Solution of the General Covering Problem," Proceedings of the Fifth International Symposium on Information Processing, Yugoslavia, Bled, October 1969.
55. Michalski, R.S. and B.H. McCormick, "Interval Generalization of Switching Theory," Proceedings of the Third Annual Houston Conference on Computing System Science, Houston, Texas, April 1971, pp. 213-226.
56. Mitchell, Owen, Charles Myers, and William Boyne, "A Max-Min Measure for Image Texture Analysis," IEEE Transactions on Computers, Vol. C-25, No. 4, April 1977, pp. 408-414.
57. Mitchell, O.R. and S.G. Carlton, "Image Segmentation Using a Local Extrema Texture Measure," Special Issue of Pattern Recognition, June 1977.
58. Müller, W., "The Leitz Texture Analyzes Systems," Leitz Scientific and Technical Information, Supplement I, 4, April 1974, Wetzlar, Germany, pp. 101-116.
59. Müller, W. and W. Herman, "Texture Analyzes Systems," Industrial Research, November 1974.
60. Ohlander, R., "Analysis of Natural Scenes," Ph.D. Dissertation, Carnegie Mellon University, Pittsburgh, Pennsylvania, 1975.
61. O'Neill, E., "Spatial Filtering in Optics," IRE Transactions on Information Theory, Vol. 2, No. 6, June 1956, pp. 56-65.

62. Osman, M.O.M. and T.S. Saukar, "The Measurement of Surface Texture by Means of Random Function Excursion Techniques," Advances in Test Measurement, Vol. 12 - Proceedings of the 21st International Instrumentation Symposium, published by the Instrument Society of America, Pittsburgh, Pennsylvania, 1975.
63. Peucker, T. and D. Douglas, "Detection of Surface-Specific Points by Local Parallel Processing of Discrete Terrain Elevation Data," Computer Graphics and Image Processing, Vol. 4, No. 4, December 1975, pp. 375-387.
64. Pickett, R.M., "Visual Analyses of Texture in the Detection and Recognition of Objects," Picture Processing and Psychopictorics, Lipkin and Rosenfeld (Editors), Academic Press, New York, 1970, pp. 289-308.
65. Pressman, Norman J., "Markovian Analysis of Cervical Cell Images," The Journal of Histochemistry and Cytochemistry, Vol. 24, No. 1, 1976 pp. 138-144.
66. Preston, K., Coherent Optical Computers, McGraw-Hill Book Company, New York, 1972.
67. Read, J.S. and S.N. Jayaramamurthy, "Automatic Generation of Texture Feature Detectors," IEEE Transactions on Computers, Vol. C-21, No. 7, July 1972, pp. 803-812.
68. Rosenfeld, Azriel, "Automatic Recognition of Basic Terrain Types on Aerial Photographs," Photogrammetric Engineering, Vol. 28, 1962, pp. 155-132.
69. Rosenfeld, Azriel, "Connectivity in Digital Pictures," Journal of the Association for Computing Machinery, Vol. 17, No. 1, January 1970, pp. 146-160.
70. Rosenfeld, Azriel, "A Note on Automatic Detection of Texture Gradients," IEEE Transactions on Computers, Vol. C-23, No. 10, October 1975, pp. 988-991.
71. Rosenfeld, Azriel and Larry Davis, "A Note on Thinning," IEEE Transactions on Systems, Man, and Cybernetics, Vol. SMC-6, No. 3, March 1976, pp. 226-228.
72. Rosenfeld, A. and A. Goldstein, "Optical Correlation for Terrain Type Discrimination," Photogrammetric Engineering, Vol. 30, 1964, pp. 639-646.
73. Rosenfeld, A. and B.S. Lipkin, "Texture Synthesis," Picture Processing and Psychopictorics, Lipkin and Rosenfeld (Editors), Academic Press, New York, 1970, pp. 309-345.
74. Rosenfeld, Azriel and John Pfaltz, "Sequential Operations in Digital Picture Processing," Journal of the Association for Computing Machinery, Vol. 13, No. 4, October 1966, October 1966, pp. 471-494.
75. Rosenfeld, Azriel and John Pfaltz, "Distance Functions on Digital Images," Pattern Recognition, Vol. 1, No. 1, 1968, pp. 33-61.
76. Rosenfeld, A. and M. Thurston, "Edge and Curve Detection for Visual Scene Analysis," IEEE Transactions on Computers, Vol. C-20, No. 5,
77. Rosenfeld, Azriel and Eleanor Troy, "Visual Texture Analysis," Technical Report 70-116, University of Maryland, College Park, Maryland, June 1970. Also in Conference Record for Symposium on Feature Extraction and Selection in Pattern Recognition (IEEE Publication 70C-51C), Argonne, Illinois, October 1970, pp. 115-124.
78. Serra, J., "Theoretical Bases of the Leitz Texture Analyses System," Leitz Scientific and Technical Information, Supplement I, 4, April 1974, Wetzlar, Germany, pp. 125-136.
79. Serra, J., "One, Two, Three, . . . , Infinity," Quantitative Analysis of Microstructures in Materials Science, Biology, and Medicine, J.L. Chernant (Editor), Dr. Riederer-Verlag GmbH, Stuttgart, 1978, pp. 9-24.
80. Serra, J. and G. Verchery, "Mathematical Morphology Applied to Fibre Composite Materials," Film Science and Technology, Vol. 6, 1973, pp. 141-158.
81. Shulman, A.R., Optical Data Processing, John Wiley & Sons, Inc., New York, 1970.
82. Stefanelli, R. and A. Rosenfeld, "Some Parallel Thinning Algorithms for Digital Pictures," Journal of the Association for Computing Machinery, Vol. 18, No. 2, April 1971, pp. 255-264.
83. Sutton, R. and E. Hall, "Texture Measures for Automatic Classification of Pulmonary Disease," IEEE Transactions on Computers, Vol. C-21, No. 2, 1972, pp. 667-676.
84. Swanlund, G., "Honeywell's Automatic Tree Species Classifier," Honeywell Systems and Research Division, Report 9D-G-24, December 31, 1969.
85. Tomita, F., M. Yachida, and S. Tsuji, "Detection of Homogeneous Regions by Structural Analysis," Proceedings of the Third International Joint Conference on Artificial Intelligence, 1973, pp. 564-571.
86. Toriwaki, J. and T. Fukumura, "Extraction of Structural Information from Grey Pictures," Computer Graphics and Image Processing, Vol. 7, No. 1, 1978, pp. 30-51.
87. Tou, J.T. and Y.S. Chang, "An Approach to Texture Pattern Analysis and Recognition," Proceedings of the 1976 IEEE Conference on Decision and Control, 1976.
88. Tou, J.T. and Y.S. Chang, "Picture Understanding by Machine Via Textural Feature Extraction," Proceedings of the 1977 IEEE Conference on Pattern Recognition and Image Processing, Troy, New York, June 1977.
89. Tou, J.T., D.B. Kao, and Y.S. Chang, "Pictorial Texture Analysis and Synthesis," Third International Joint Conference on Pattern Recognition, Coronado, California, August 1976.
90. Triendl, E.E., "Automatic Terrain Mapping by Texture Recognition," Proceedings of the Eighth International Symposium on Remote Sensing of Environment, Environmental Research Institute

of Michigan, Ann Arbor, Michigan, October 1972.

91. Tsuji, S. and F. Tomita, "A Structural Analyzer for a Class of Textures," Computer Graphics and Image Processing, Vol. 2, 1973, pp. 216-231.
92. Weszka, J., C. Dyer, and A. Rosenfeld, "A Comparative Study of Texture Measures for Terrain Classification," IEEE Transactions on Systems, Man, and Cybernetics, Vol. SMC-6, No. 4, April 1976, pp. 269-285.
93. Wied, G., G. Bahr, and P. Bartels, "Automatic Analysis of Cell Images," Automated Cell Identification and Cell Sorting, Wied and Bahr (Editors), Academic Press, New York, 1970, pp. 195-360.
94. Woods, J.W., "Two-Dimensional Discrete Markovian Fields," IEEE Transactions on Information Theory, Vol. IT-18, No. 2, March 1972, pp. 232-240.
95. Yaglom, A.M., Theory of Stationary Random Functions, Prentice-Hall, Inc., New Jersey, 1962.
96. Yokoi, S., J. Toriwaki, and T. Fukumura, "An Analysis of Topological Properties of Digitized Binary Pictures Using Local Features," Computer Graphics and Image Processing, 4, 1975, pp. 63-73.
97. Zucker, S., On the Foundations of Texture: A Transformational Approach, Technical Report TR-331, University of Maryland, College Park, Maryland, September 1974.
98. Zucker, S.W., "Toward a Model of Texture," Computer Graphics and Image Processing, Vol. 5, No. 2, 1976, pp. 190-202.
99. Zucker, S.W., A. Rosenfeld, and L. Davis, "Picture Segmentation by Texture Discrimination," IEEE Transactions on Computers, Vol. C-24, No. 12, December 1975, pp. 1228-1233.



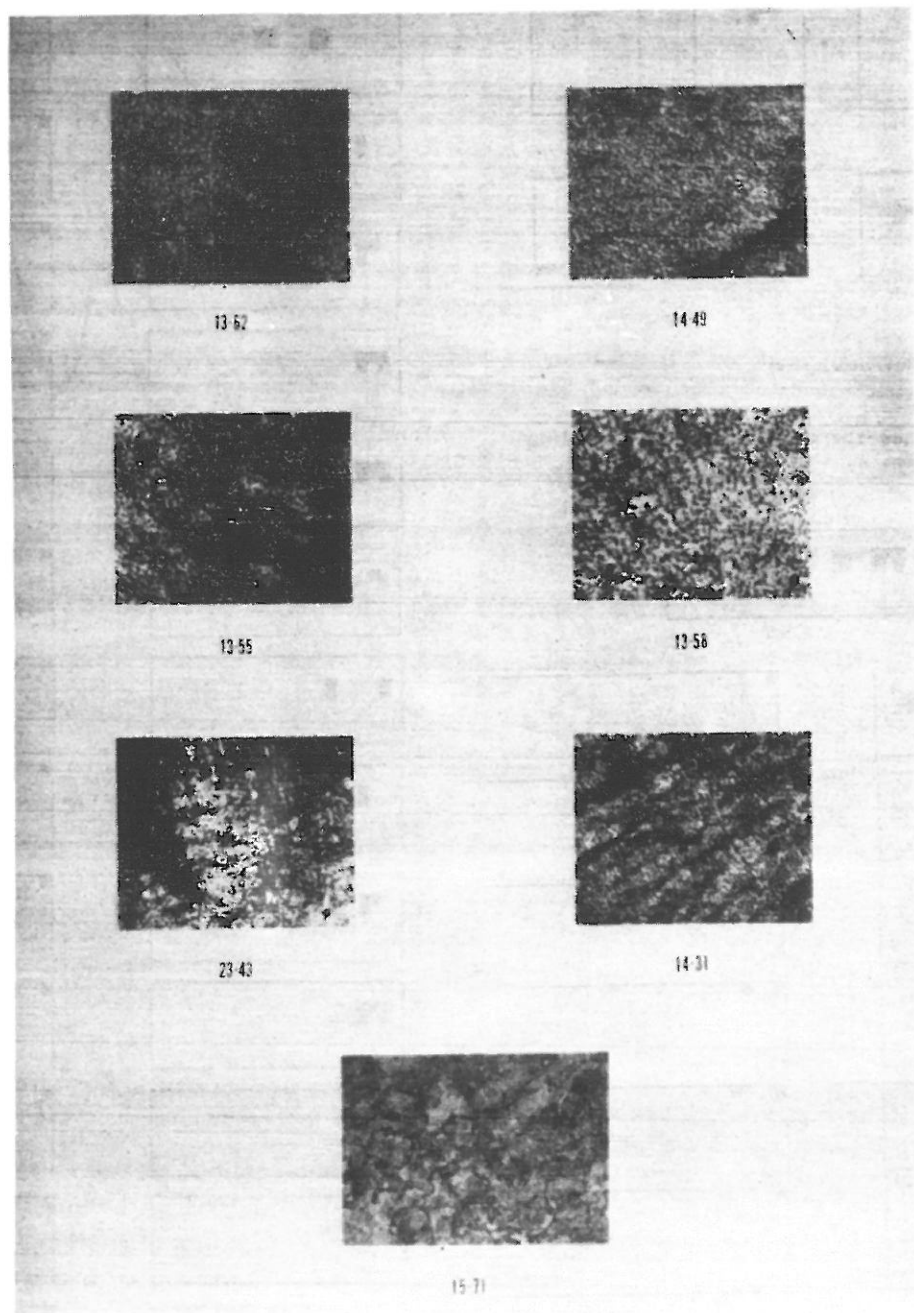
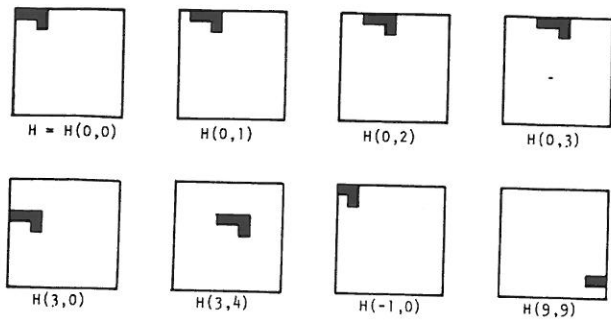


Figure 1 illustrates some of the image textures used by Kaizer in his autocorrelation experiment (taken from Kaizer, 1955).



$$H = \{(0,0), (0,1), (0,2), (1,2)\}$$

Figure 2 illustrates the set H and some of its translates.

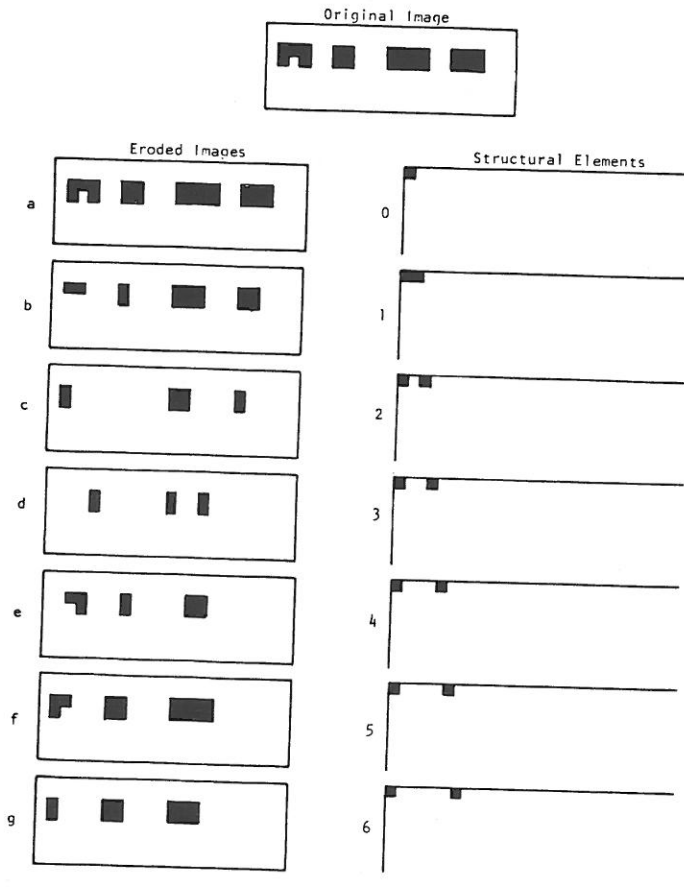


Figure 3 illustrates the erosion operation for a number of different structural elements on the same image.

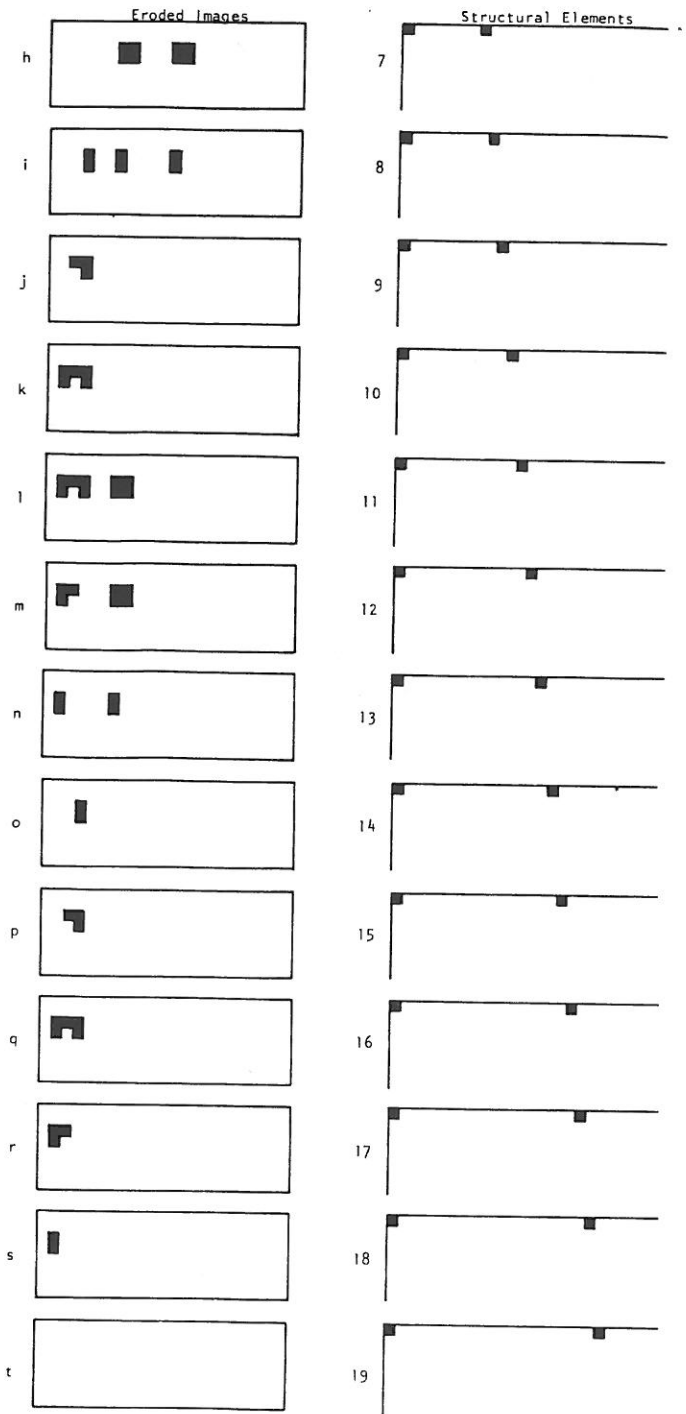


Figure 3 (continued).

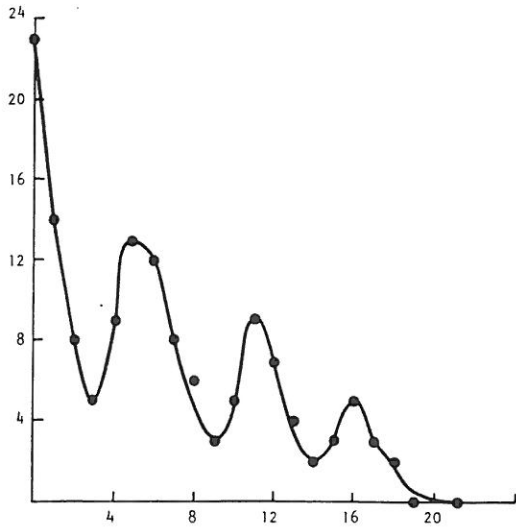


Figure 4 illustrates the covariance function in the horizontal direction for the image in Figure 3.

(1,1)	(1,2)	(1,3)	(1,4)
(2,1)	(2,2)	(2,3)	(2,4)
(3,1)	(3,2)	(3,3)	(3,4)
(4,1)	(4,2)	(4,3)	(4,4)

$$L_y = \{1, 2, 3, 4\}$$

$$L_x = \{1, 2, 3, 4\}$$

$$R_H = \{(k,l), (m,n) \in (L_y \times L_x) \times (L_y \times L_x) \mid k-m=0, |l-n|=1\}$$

$$= \{(1,1), (1,2), (1,2), (1,1), (1,2), (1,3), (1,3), (1,2), (1,3), (1,4), (1,4), (1,3), (2,1), (2,2), (2,2), (2,1), (2,2), (2,3), (2,3), (2,2), (2,3), (2,4), (2,4), (2,3), (3,1), (3,2), (3,2), (3,1), (3,2), (3,3), (3,3), (3,2), (3,3), (3,4), (3,4), (3,3), (4,1), (4,2), (4,2), (4,1), (4,2), (4,3), (4,3), (4,2), (4,3), (4,4), (4,4), (4,3)\}$$

Figure 5 illustrates the set of all distance 1 horizontal neighboring resolution cells on a 4 x 4 image.

0	0	1	1
0	0	1	1
0	2	2	2
2	2	3	3

Figure 6-a.

		Grey Tone			
		0	1	2	3
Grey Tone	0	#(0,0)	#(0,1)	#(0,2)	#(0,3)
	1	#(1,0)	#(1,1)	#(1,2)	#(1,3)
	2	#(2,0)	#(2,1)	#(2,2)	#(2,3)
	3	#(3,0)	#(3,1)	#(3,2)	#(3,3)

Figure 6-b. This shows the general form of any gray tone spatial dependence matrix for an image with integer gray tone values 0 to 3. #(i,j) stands for number of times gray tones i and j have been neighbors.

$$0^\circ \quad P_H = \begin{pmatrix} 4 & 2 & 1 & 0 \\ 2 & 4 & 0 & 0 \\ 1 & 0 & 6 & 1 \\ 0 & 0 & 1 & 2 \end{pmatrix}$$

Figure 6-c.

$$90^\circ \quad P_V = \begin{pmatrix} 6 & 0 & 2 & 0 \\ 0 & 4 & 2 & 0 \\ 2 & 2 & 2 & 2 \\ 0 & 0 & 2 & 0 \end{pmatrix}$$

Figure 6-d.

$$135^\circ \quad P_{LD} = \begin{pmatrix} 2 & 1 & 3 & 0 \\ 1 & 2 & 1 & 0 \\ 3 & 1 & 0 & 2 \\ 0 & 0 & 2 & 0 \end{pmatrix}$$

Figure 6-e.

$$45^\circ \quad P_{RD} = \begin{pmatrix} 4 & 1 & 0 & 0 \\ 1 & 2 & 2 & 0 \\ 0 & 2 & 4 & 1 \\ 0 & 0 & 1 & 0 \end{pmatrix}$$

Figure 6-f.

Figure 6 illustrates the spatial co-occurrence calculations. (Take from Haralick et al.<sup>33</sup>).

Uniformity or energy  
(Related to the variance of  
{ $P_{i1}, \dots, P_{ij}, \dots, P_{iN}$ })

$$\sum_{i,j} P_{ij}^2$$

Entropy

$$\sum_{i,j} P_{ij} \log P_{ij}$$

Maximum probability

$$\max_{i,j} P_{ij}$$

Contrast

$$\sum_{i,j} |i-j|^k (P_{ij})^k$$

Inverse difference moment

$$\sum_{i,j} \frac{(P_{ij})^2}{|i-j|^k}$$

Correlation

$$\sum_{i,j} \frac{(i-u)(j-u)P_{ij}}{\sigma^2}$$

Probability of a run of length n for gray tone i

$$\frac{(P_i - P_{ii})^2 (P_{ii})^{n-1}}{P_i^n}$$

$$\text{where } P_i = \sum_j P_{ij}$$

Figure 7 lists 7 of the common features computed from the co-occurrence probabilities.

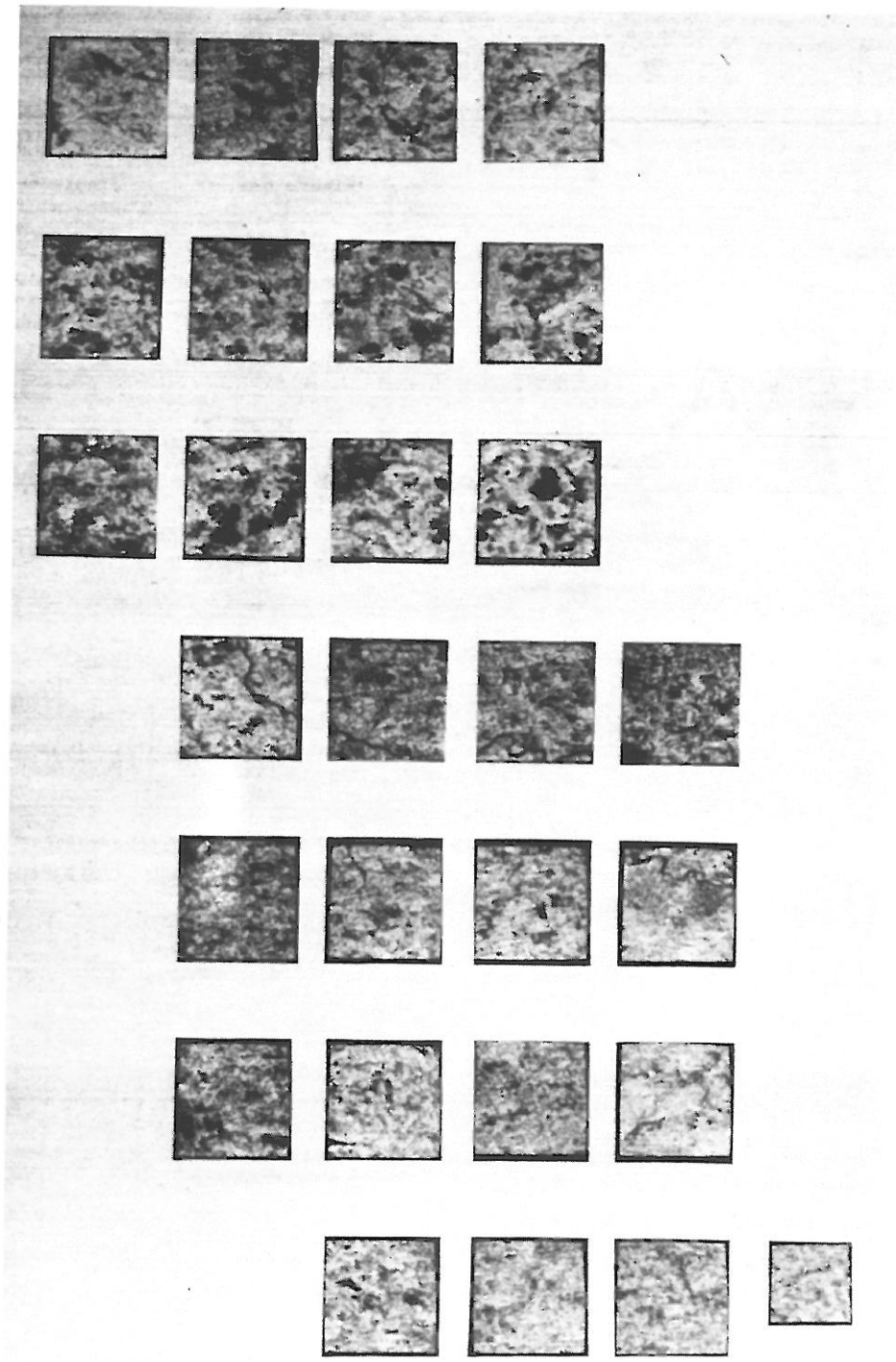


Figure 8 illustrates computer generated subimages in the test area.

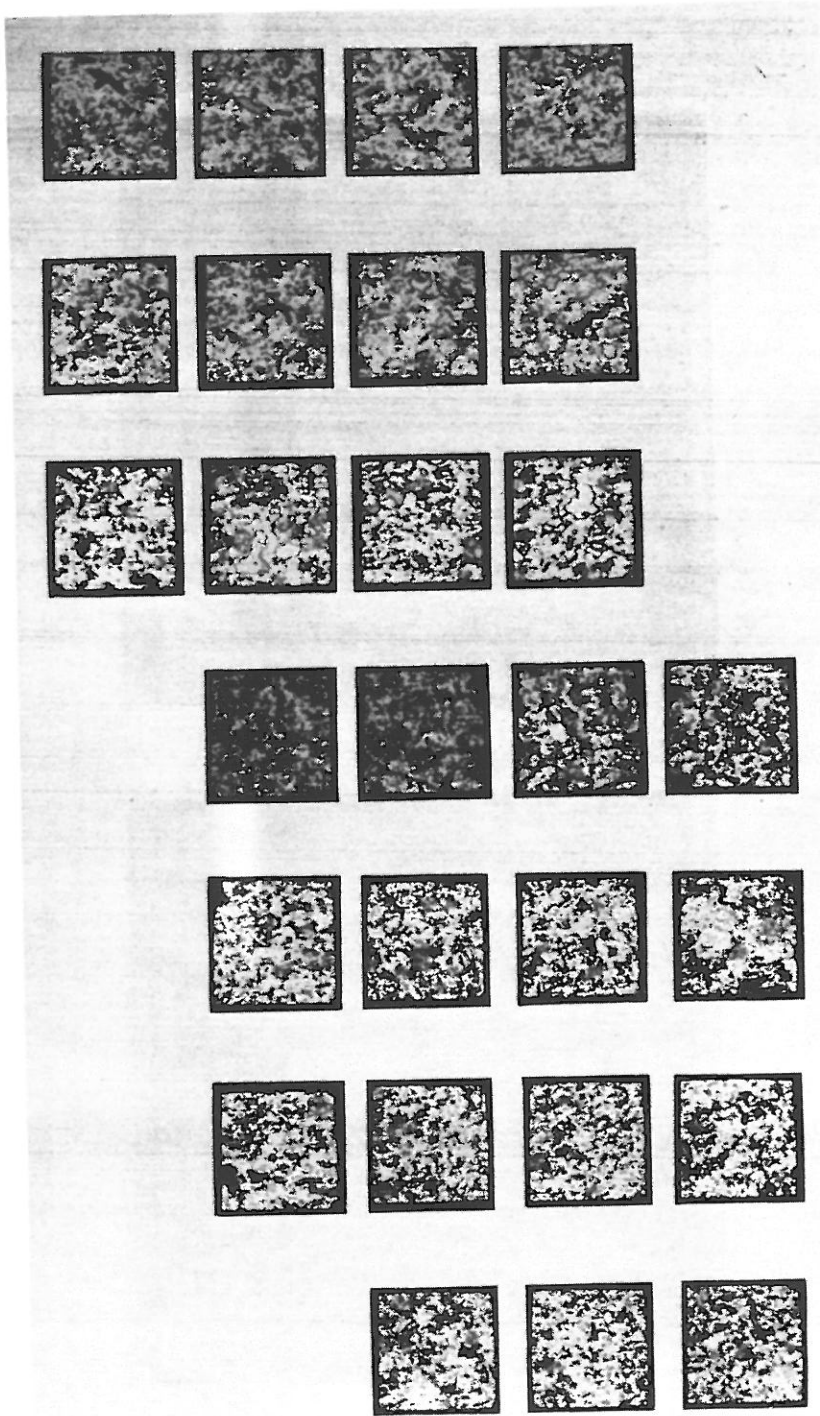


Figure 9 illustrates the textural transforms of the subimages of Figure 8.

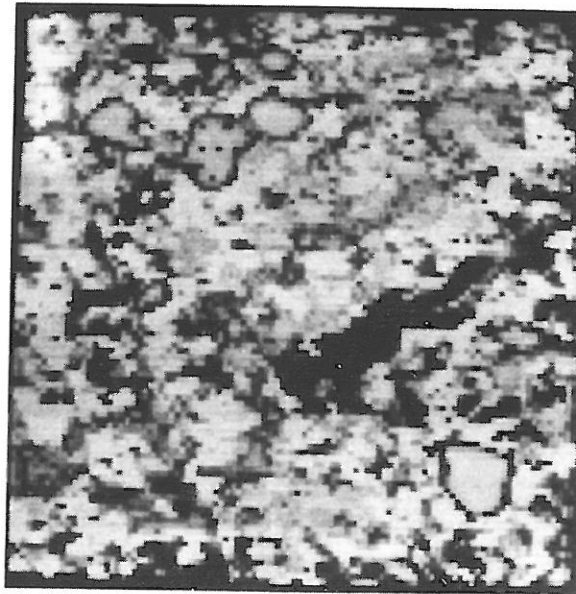
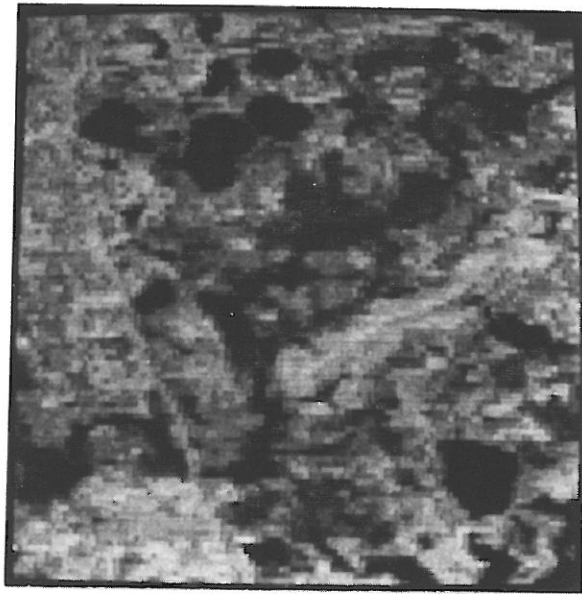


Figure 10 illustrates an enlargement of subimage (1,3) and its transform.

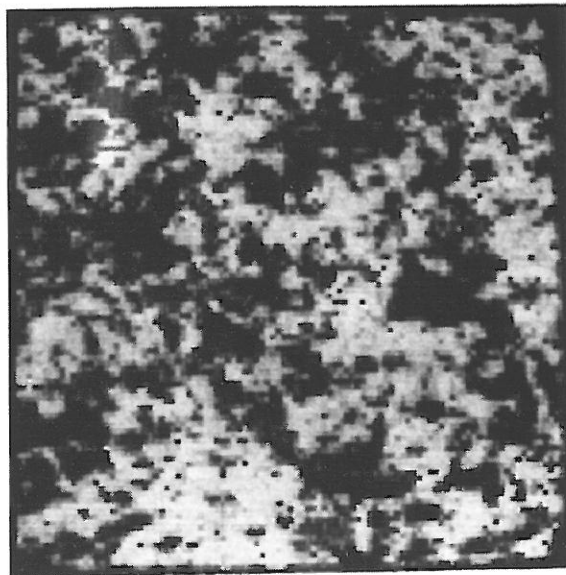
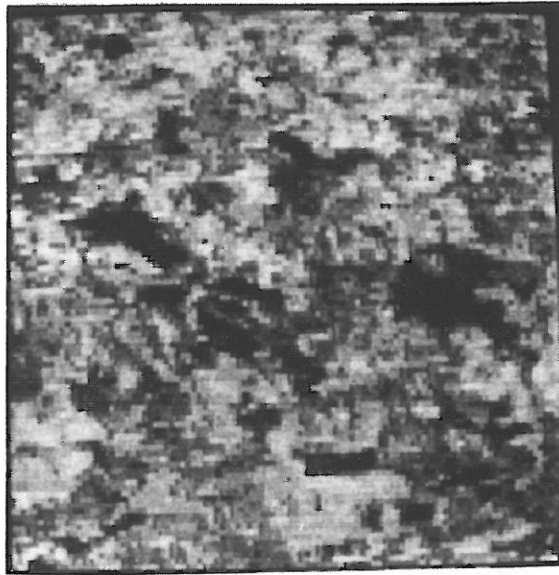
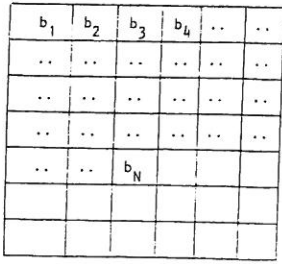
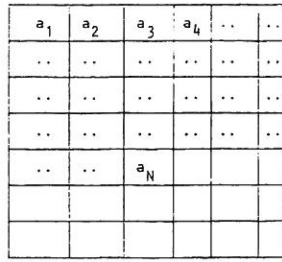


Figure 11 illustrates an enlargement of subimage (6,0) and its transform.



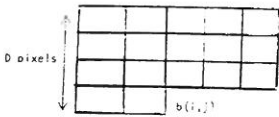
Randomly Generated Noise Image



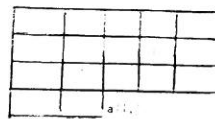
Synthesized Image

$$a_{N+1} = \underbrace{\sum_{k=0}^{K-1} \alpha_k a_{N-k}}_{\text{Auto-Regressive Terms}} + \underbrace{\sum_{\ell=0}^{L-1} \beta_\ell b_{N-\ell}}_{\text{Moving Average Terms}}$$

Figure 12 illustrates how from a randomly generated noise image and a given starting sequence  $a_1, \dots, a_K$ , representing the initial boundary conditions, all values in a texture image can be synthesized by a one-dimensional auto-regressive model.



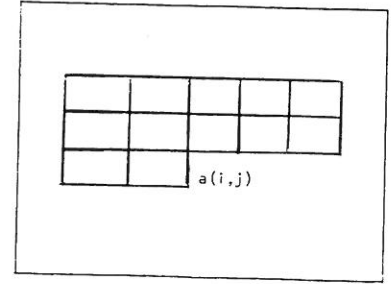
Order-D Neighborhood of Randomly Generated Noise Image



Order-D Neighborhood of Synthesized Image

$$a(i,j) = \underbrace{\sum_{(k,\ell) \in N(i,j)} \alpha(i-k, j-\ell) a(k,\ell)}_{\text{Auto-Regressive Terms}} + \underbrace{\sum_{(k,\ell) \in N(i,j)} \beta(i-k, j-\ell) b(k,\ell)}_{\text{Moving Average Terms}}$$

Figure 13 illustrates how from a randomly generated noise image and a given starting sequence for the first order-D neighborhood in the image, all values in a texture image can be synthesized by a two-dimensional auto-regressive model.



$$\hat{a}(i,j) = \underbrace{\sum_{(k,\ell) \in N(i,j)} \alpha(i-k, j-\ell) a(k,\ell)}_{\text{Auto-Regressive Terms}}$$

$$+ \underbrace{\sum_{(k,\ell) \in N(i,j)} \beta(i-k, j-\ell) [a(k,\ell) - \hat{a}(k,\ell)]}_{\text{Moving Average Terms}}$$

Figure 14 illustrates how a gray tone value for pixel (i,j) can be estimated using the gray tone values in the neighborhood  $N(i,j)$  and the differences between the actual values and the estimated values in the neighborhood.

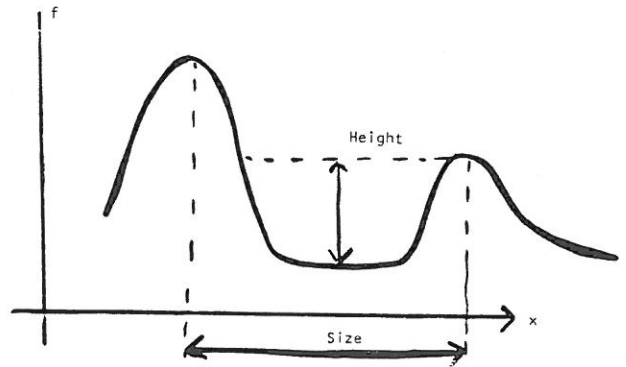


Figure 15 illustrates how the height and size properties of a valley are defined.



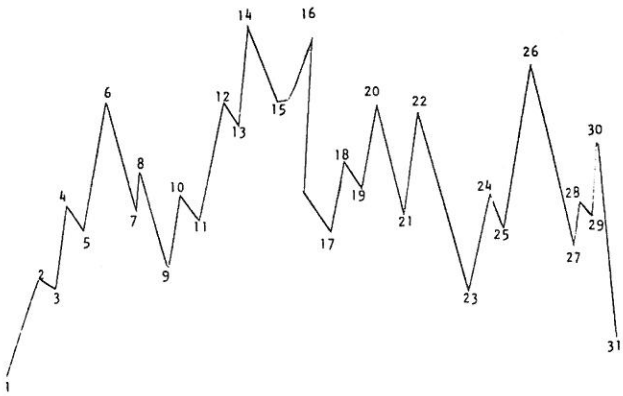


Figure 16 illustrates a waveform.

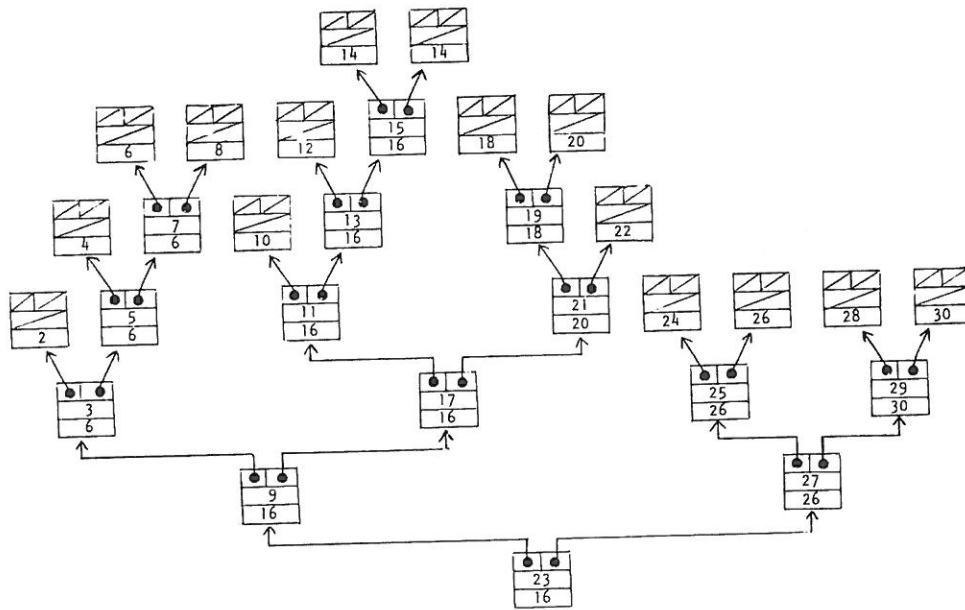


Figure 17 illustrates Ehrlich and Foith's relational tree for the waveform of Figure 16. The first number in each node is the lowest valley point. The second number is the highest peak point for the segment.

